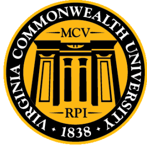

Virginia Commonwealth University
VCU Scholars Compass

Theses and Dissertations | Graduate School

2012

Thermal Quenching of Photoluminescence from GaN

Anita Olsen
Virginia Commonwealth University

Follow this and additional works at: https://scholarscompass.vcu.edu/etd

Part of the Physics Commons

© The Author

Downloaded from
https://scholarscompass.vcu.edu/etd/2796

This Thesis is brought to you for free and open access by the Graduate School at VCU Scholars Compass. It has been accepted for inclusion in Theses and Dissertations by an authorized administrator of VCU Scholars Compass. For more information, please contact libcompass@vcu.edu.

المنارة للاستشارات

www.manaraa.com

Thermal Quenching of Photoluminescence from GaN

A thesis submitted in partial fulfillment of the requirements for the degree of Master of Science in Physics / Applied Physics at Virginia Commonwealth University.

By

Anita J. Olsen

B.S. in Physics

Minor in Mathematical Sciences

Virginia Commonwealth University, 2010

M.S. in Physics/Applied Physics

Virginia Commonwealth University, 2012

Director: Michael A. Reshchikov, Associate Professor, Department of Physics

Virginia Commonwealth University,

Richmond, Virginia, 23284

April 20, 2012

المنارة للاستشارات

www.manaraa.com

Acknowledgments

This thesis is dedicated to all of the people in my life that have given me support, love, and guidance. I cannot begin to express my gratitude for my family, my friends and the members of the VCU physics department that have helped me along this journey.

I would like to personally thank Dr. Glen MacLachlan for introducing me to the world of physics. It was the knowledge and experiences that I gained from him along with his enthusiasm and encouragement that started my passion for physics.

This passion has continued to flourish with the help of several members of the VCU physics department. I have received a tremendous amount of compassion and support from the people here that have led to the success of this thesis and my success in life as a whole. A special thanks goes to Dr. Alison Baski for the major role she played in my positive and uplifting experience here. She is an inspiration to me and I have a great deal of respect and admiration for her. I would also like to thank Dr. Marilyn Bishop and Dr. Tom McMullen for seeing my potential and giving me so much assistance, support, and knowledge. Dr. Bishop is an amazing woman and has become more than a professor to me; she will always be dear to my heart. Another person that deserves a great deal of gratitude is Dr. Michael Reshchikov. It was a privilege to have such a brilliant man as an advisor and I am grateful for the immense amounts of wisdom I have gained from him. I am also very appreciative of his dedication and patience with me during my collegiate career at VCU.

Many more deserve thanks and to those I have not mentioned here, you are not forgotten and I thank you!

المنارة للاستشارات

www.manaraa.com

Table of Contents

Acknowledgments .... *ii*

List of Figures .... *v*

Abstract .... *ix*

Introduction *1*

Chapter 1. Literature Review *3*

1.1 Gallium Nitride 3

1.2 Growth of GaN 4

1.3 Point Defects 8

1.4 Photoluminescence from defects in GaN 14

1.4.1 PL bands in GaN 14

1.4.2 Effects of Temperature in GaN 19

1.4.3 Effects of Excitation in GaN 23

Chapter 1 Figures 26

Chapter 2. Experimental Details *33*

2.1 Sample 33

2.2 Experimantal Set-Up 33

Chapter 2 Figures 37

Chapter 3. Experimental Results *39*

3.1 Low Temperature PL Spectra if Zn-doped and Undoped Gan 39

3.2 The Effect of Temperature on PL Intensity 40

3.3 The Effect of Excitation on PL Intensity 45

Chapter 3 Figures 47

المنارة للاستشارات

www.manaraa.com

Chapter 4. Theory and Experimental Comparison *55*

4.1 Rate Equations Model 55

4.2 Abrupt Tunable Quenching of PL 61

Chapter 4 Figures 63

Chapter 5. Comparison of Theory with Experiment *64*

Chapter 5. Figures 66

Chapter 6. Summary *67*

References *69*

Appendix: Mathematica Program *71*

المنارة للاستشارات

www.manaraa.com

List of Figures

Fig. 1-1: Wurtzite crystal structure of GaN. The larger yellow atoms are Ga and the smaller white atoms are N. (http://en.wikipedia.org/wiki/File:Wurtzite_polyhedra.png) 26

Fig. 1-2: Schematic illustration for GaN HVPE growth: 1 – main reactor tube, 2 – heating elements, 3 – Ga source gas channel, 4 – boat with Ga Melt, 5 – Ga melt, 6 – substrate, 7 – substrate holder, and 8 – ammonia source tube. (www.oxford-instruments.com/products/etching.../hvpe.aspx) 26

Fig. 1- 3: Schematic illustration for MOVPE growth. Face-down multiwafer set-up, gear driven rotation, separated flow of active species (courtesy EMC, Japan). 27

Fig. 1-4: Schematic illustration for MBE growth. A simple sketch that shows the main components, rough layout and concept of the main chamber. (http://en.wikipedia.org/wiki/File:MBE.png).. 27

Fig. 1-5: Formation energies for native point defects in GaN as a function of Fermi level. The zero of the Fermi level represents the top of the valence band. Only segments related to the lowest-energy states are shown and their slopes indicate their charge state. The transition between charge states can be seen in the kinks of the curves.[12] 28

Fig. 1-6: Transition levels that were determined from Fig. 1-5 for defects in GaN.[10]................. 28

Fig. 1-7: Photoluminescence spectra of undoped GaN of several implanted elements at 78° K.[13] 29

Fig. 1-8: Formation energy as a function of Fermi level for native defects (nitrogen and gallium vacancies) and impurity donors (oxygen and silicon) in GaN in gallium-rich conditions.[12]. 30

www.manaraa.com

Fig. 1-9: Formation energy as a function of Fermi level for magnesium in different configurations along with the native defect of a nitrogen vacancy and hydrogen interstitial in gallium-rich conditions.[12] 30

Fig. 1-10: PL spectra from undoped GaN at 15 K. The spectra are plotted in logarithmic scale and displaced vertically for better viewing.[10] 31

Fig. 1-11: Calculated temperature dependencies of the QE for radiative recombination channels in GaN of excitons and two acceptor channels (A1 and A2).[19] 31

Fig. 1- 12: Low-temperature PL spectra at different excitation intensities of a Mg-doped GaN sample.[26] 32

Fig. 2-1: Simplified view of experimental set-up for photoluminescence experiments........ 37

Fig. 2-2: Diagram of a Czerny-Turner monochromator (http://en.wikipedia.org/wiki/File:Czerny-turner.png). 37

Fig. 2-3: Schematic of a photomultiplier tube (PMT) (http://en.wikipedia.org/wiki/File:Photomultipliertube.svg)........ 38

Fig. 2- 4: Typical temperature characteristics of Dark Current at 1000 V, after 30 min storage in darkness. (www.hamamatsu.com) 38

Fig. 3-1: PL Spectra from undoped (sample th1011) and Zn-doped GaN (ap274) at a temperature of 13 K and P_{exc} = 0.002 W/cm^2. The Zn-doped data has been multiplied by 0.3. 47

Fig. 3-2: PL Spectra of a Zn-doped GaN (sample ap274) at a temperature of 15 K and P_{exp} = 0.3 W/cm^2........ 47

Fig. 3-3: Temperature dependence of the BL band quantum efficiency in undoped GaN (th1011, blue squares) and Zn-doped GaN (s452 , red triangles)........ 48

المنارة للاستشارات

www.manaraa.com

Fig. 3-4: PL spectra of Zn-doped GaN (ap274) in the temperature range of 15 to 325 K with P_{exc} = 0.3 W/cm^2. 48

Fig. 3-5: PL spectra of the excitonic luminescence band and its LO phonon replica in the temperature range of 15 K to 230 K at P_{exc} = 0.3 W/cm^2. 49

Fig. 3-6: PL spectra of the UVL band and its LO phonon replica in the temperature range of 15 K to 230 K at P_{exc} = 0.3 W/cm^2. 49

Fig. 3-7: PL spectra of Zn-doped GaN (ap274) in the temperature range of 15 to 320 K with P_{exc} = 12.2 W/cm^2. 50

Fig. 3-8: PL spectra of the excitonic luminescence band, UVL band and their LO phonon replicas in the temperature range of 13 K to 230 K at P_{exc} = 12.2 W/cm^2. 50

Fig. 3-9: PL spectra of Zn-doped GaN (ap274) in the temperature range of 15 to 280 K with P_{exc} = 0.00027 W/cm^2. 51

Fig. 3-10: PL spectra of the excitonic luminescence band, UVL band and their LO phonon replicas in the temperature range of 13 K to 300 K at P_{exc} = 0.00027 W/cm^2. 51

Fig. 3-11: PL spectra of Zn-doped GaN (ap274) at the temperature of 13 K with excitation intensity ranging from 0.3 to 0.00003 W/cm^2 52

Fig. 3-12: PL spectra of the excitonic luminescence band and its LO phonon replica in the excitation intensity range of 0.3 to 0.00003 W/cm^2. 52

Fig. 3-13: PL spectra of the UVL band and its LO phonon replica in the excitation intensity range of 0.3 to 0.00003 W/cm^2. 53

Fig. 3-14: PL spectra of Zn-doped GaN (sample ap274) at excitation intensities of 12.2, 0.3 and 0.00027 W/cm^2. 53

المنارة للاستشارات

www.manaraa.com

Fig. 3-15:Fig. 3-15: Quantum efficiency of the BL band for Pexc from 12.2 **4o 2.6 × 10-7 W/cm2..**
.... 54

Fig. 4-1: Basic band diagram and main transitions of electrons for a semiconductor with a shallow donor (*D*), acceptor (*A*), and a nonradiative deep donor (*S*)................................... 63

Fig. 5-1: Theoretical fit with experimental data for Pexc of 12.2, 0.3 and 0.00027 W/cm2. Parameters for fit were *NA* = 9.35 × 1016, *NS* = 8.5 × 1016, *ND* = 8.5 × 1015 (all in cm-3); *CnS* =10-7, *CnD* = 10-8, *CpS* = 5 × 10-7, *CpA* = 10-6, *CnA* = 10-11, *CDA* = 10-11 (all in cm3/s) and *ED* = 30 meV, *EA* = 340 meV. 66

www.manaraa.com

Abstract

By Anita J. Olsen

A thesis submitted in partial fulfillment of the requirements for the degree of Master of Science at Virginia Commonwealth University. Virginia Commonwealth University, 2012.

Major Director: Michael A. Reshchikov, Associate Professor, Department of Physics

GaN is a III-V semiconductor that is a promising material used in production of light emitting devices and high power/high frequency electronics. The electronic and optical properties of GaN are subdued by defects that occur during the growth processes of this material. The emitted photoluminescence (PL) from optically excited GaN gives insight into the origins and effects of point defects within the crystal lattice structure of GaN. In this study, PL spectroscopy is used to examine and analyze the point defects that occur in Zn-doped GaN. The blue luminescence band seen in undoped and Zn-doped GaN have identical fine structure and properties. This band is attributed to a Zn_{Ga} acceptor. In Zn-doped, the PL intensity quenches abruptly at certain temperatures, which increase with increasing excitation intensity. This behavior is different from the PL quenching in undoped GaN. The PL behavior was simulated with a phenomenological model based on rate equations. A program created with mathematical modeling software, in conjunction with the basic rate equations, was used to explain the unusual behavior of the abrupt thermal quenching observed in Zn-doped GaN.

للاستشارات المنارة
www.manaraa.com

Introduction

Gallium nitride has become one of the most important semiconductor materials and is used in a variety of devices such as light emitting diodes (LED) and blue-ray/DVD players. There is a high diversity of future prospects for this advantageous material due to its wide bandwidth and its chemical and structural stability that withstands high voltages, high heat and radiation. It is important to understand the mechanisms involved within this material to improve the quality and decrease or utilize the effects of naturally occurring or purposefully introduced impurities to enhance efficiency of light-emitting devices and performance of electrical devices.

In the growth process of GaN, there are several factors that produce point defects within the material. These point defects are a result of nonequilibrium conditions during the growth process and contamination of the sources used. It is important to study these effects of these defects to determine their origin and concentrations, which will lead to the improvement of the growth methods used in creating GaN. In the attempt to make a conductive *n*-type or *p*-type GaN, there are also purposefully introduced point defects that result from doping. It is also important to understand the dynamics involved with this introduction of impurities, so that enhancements to this material can be utilized and future prospects realized.

Several of the effects related to point defects can be observed using luminescence experiments. Photoluminescence (PL) spectroscopy is a nondestructive method used to investigate the electronic structure of materials. This method is widely used in the study of GaN because of the intensity of luminescence that occurs in the visible range of the spectrum. The spectra that are obtained from PL experiments contain information on the types of defects involved, along with their contribution to the functionality of GaN.

المنارة للاستشارات
www.manaraa.com

One notable phenomenon observed in PL experiments is the quenching of different bands in the spectrum as temperature is increased. This thermal quenching gives additional information about the point defects involved in this luminescence. Usually, the PL intensity decreases with increase in temperature, and the slope of this decrease allows one to determine the activation energy for these defects. The additional information obtained in the observation of thermal quenching can help with characterization and understanding the properties of the defects involved along with understanding the electrical and optical effects they incur.

Understanding the functionality of GaN and its properties is of great importance for the advancement of this material. It has already proved to be a superior semiconductor material and is being utilized in some of the most technologically advanced devices. The improvement of this material can further advance its usefulness in applications but these improvements can only be made with clearer understanding of its functionality. This understanding can be greatly enhanced with the observation and analysis of its mechanisms with the use of photoluminescence experiments.

المنارة للاستشارات
www.manaraa.com

Chapter 1. Literature Review

1.1 Gallium Nitride

GaN is a binary III/V semiconductor that has a direct bandgap of 3.4 eV at room temperature and is commonly used for light-emitting diodes (blue and ultraviolet). It is a very hard compound with a Wurtzite crystal structure, seen in Fig. 1-1, that is resistant to cracking in its pure form.[1] GaN has a high melting point of 2500° C and is chemically and structurally stable. The diodes made from this material are faster, smaller in size, lower in energy consumption, and have a longer lifetime than incandescent light sources. GaN is used to produce violet (405 nm) laser diodes that are used for data storage in high-definition blue-ray/DVD devices. Previous DVD devices used lasers in the visibly red, near infrared region, of the spectrum (780 nm), storing only a fourth of the information that the GaN devices can store. GaN devices have shown stability in radiation environments due to a low sensitivity to ionization radiation. This is a choice material for military and space applications, including satellites, along with use in solar cell arrays.[2]

GaN-based transistors are used for amplifying or switching electronic signals. GaN is a preferred semiconductor in power amplifiers at microwave frequency in comparison with gallium arsenide because it can withstand higher temperatures and voltages. There are several potential market applications for this semiconductor material including high-voltage switching devices for power grids and GaN-based RF transistors in place of magnetrons in microwave ovens. Microwave radio-frequency power amplifiers based on GaN would also be useful in high-speed wireless data transmission. GaN has also gained interest as an advantageous material for

المنارة للاستشارات
www.manaraa.com

its performance in high power electronics including automotive and electric car applications as well as military electronics such as Active Electronically Scanned Array radars.[3]

Another interesting characteristic of GaN is that it is non-toxic and biocompatible, which makes it useful in the biomedical field in the research of implantable technologies. GaN is currently being studied for possible use in a variety of applications such as electrodes for neurostimulation therapies and transistors used to monitor blood chemistry. There are reports of improved adherence and cell growth on GaN surfaces versus previously studied silicon. The cells observed on etched surfaces and surfaces that were functionalized with a peptide included neurite-producing cells and there is increased cell adhesion and spreading with a covalently bound peptide. GaN is also remarkably stable in aqueous solutions and is drawing attention as an important material to study for the benefit of medical application use.[4] By acquiring a better understanding of the functions and properties of GaN, improvements can be made in the efficiency and quality of the material, which will further enhance GaN-based devices.

1.2 Growth of GaN

The development of higher quality GaN has been motivated by the progress made in understanding defects that occur from the growth process. Minimizing the defects that result from different chemical and application processes will increase the efficiency and reliability of GaN. Because GaN has a high melting temperature and a very high decomposition pressure, it cannot be grown using the conventional methods used for semiconductors such as GaAs and Si.[5] To accommodate these characteristics, nitride-based devices use epitaxial growth processes in the manufacturing process. Epitaxy is the process of depositing a monocrystalline layer over a substrate that has a crystal structure symmetry that is very similar to the deposited material. This process is called homoepitaxy if the deposition of GaN is on a GaN substrate, but if it is started

المنارة للاستشارات
www.manaraa.com

on a different substrate, it is called heteroepitaxy. The most widely used substrate for GaN epitaxy is sapphire because it is inexpensive and there have been established ways of dealing with the substrate to align it closely with the GaN crystal structure. The three main types of growth processes used for GaN are hydride vapour phase epitaxy (HVPE), molecular beam epitaxy (MBE) and metal organic vapour phase epitaxy (MOVPE).

HVPE was the first epitaxial method used for the fabrication of single GaN crystals. It was developed in the 1960's and has a high growth rate (up to 100 µm per hour) compared to MOVPE and MBE growth processes. Fig. 1-2 is a schematic illustration of the basic method of this process. The growth apparatus is encased in heating elements and contains two gas source channels in the source zone and a substrate on a substrate holder in the growth zone of a main reactor tube. In the Ga source gas channel there is a boat containing Ga metal that is introduced to a hydrochloric (HCI) gas, and the chemical reaction of the two creates a gallium chloride gas. This newly formed gas is transported into the growth zone where it reacts with ammonia from another source tube and creates GaN. Single crystal GaN is then formed on the substrate with deposition rates of several microns per minute that allows it to grow hundred micron thick layers. The only roadblock that occurred in the progress of the material quality and the understanding of the process of HPVE was the inability to produce p-type GaN because of the high background n-type carrier concentration that was prevalent in this growth method. This stunted attempts to create GaN-based blue light emitting diodes, which lead to the use of other forms of epitaxial processes. With recent advancements in the growth process, highly-resistive *n*-type or possibly *p*-type GaN has been produced using dopants in the HVPE method.

HVPE is not conducive for heterolayers and control of layer thicknesses, although it has improved considerably, but another epitaxial technology called metal organic chemical vapor

المنارة للاستشارات
www.manaraa.com

deposition (MOCVD, also called MOVPE) is. This method was utilized for producing p-type GaN materials in the early 90's. This was the first method used to make GaN-based laser diodes (LDs) and high performance electronic devices.[6] MOVPE is a chemical vapour deposition method that uses ammonia (NH_3) as a nitrogen precursor along with gallium sources such as trimethylgallium, $Ga(CH_3)_3$ (TMG), or triethylgallium, $Ga(C_2H_5)_3$ (TEG) to create GaN. It is a process that includes the simultaneous combination of heat, mass, and momentum transport along with gas-phase and surface reactions. The growth chamber used in MOVPE is designed to prevent any premature reaction of the metal alkyls and ammonia and is monitored with laser reflectrometry for real time diagnosis of the growth process. The chamber has reactor walls that use either a cold wall approach or a hot wall approach to prevent overheating. A liner made of ceramic or quartz is located between the wall and a susceptor that is made of metalorganic compounds. The chamber also holds the substrate, gas injection units and temperature control units that maintain a controlled temperature. Each individual wafer substrate is located on a separate small disc or, in newer designs, several wafers sit on a platen. These discs are either rotated as a whole or in a planetary wave to guarantee thickness and homogeneous distribution of alloy composition as seen in Fig. 1- 3. The growth of GaN on a sapphire substrate begins with a low temperature buffer layer to prevent nucleation of isolated islands. To promote a full coverage nucleation layer on the sapphire substrate, it undergoes a heat treatment at 1050° C under NH_3. This is called a nitridation step, and it forms several monolayers of AlN on top of the sapphire. The temperature is then decreased to 450-650° C and a GaN nucleation layer is deposited at a temperature of 600° C. The low temperature deposition allows higher nucleation rates because of high supersaturation, and the mobility of surface species is decreased, which promotes a uniform dispersion of atoms of reactant species to effectively cover the substrate. The

المنارة للاستشارات
www.manaraa.com

low temperature deposition is then stopped for a short annealing of the nucleation layer at the growing temperature of 1050° C and then continued for the rest of the epitaxial growth of the GaN samples.[5] A typical thickness of GaN layers grown by the MOVPE technique is 2-10 μm.

Molecular beam epitaxy (MBE) is another method for growing GaN that was developed in the late 1960's at Bell Laboratories by two American physicists, Chinese-born Alfred Y. Cho and John R. Arthur, Jr.[7] It is a high vacuum or ultra-high vacuum technique that uses a slow physical deposition rate to produce high quality epitaxial structures with monolayer control. Metallic gallium and nitrogen gas are the source materials used in MBE growth of GaN. The nitrogen gas is passed through a plasma source, which is a vital step, because the high binding energy of the N_2 molecule in its ground state prevents thermal dissociation at the film growth surface at temperatures used for MBE growth of GaN (600-800° C).[8] This activated nitrogen beam and a gallium vapor beam from an effusion cell (shown in Fig. 1-4) are directed toward a heated substrate. The heating of the substrates is typically done with the use of chucks or susceptors, and the temperature can be monitored with a thermocouple or a pyrometer.[9] Other effusion cells contain different dopants to be used in n-type or p-type GaN. There are shutters in front of each effusion cell furnace to control the thickness of each layer. The beam control from these shutters has a precision of depositing a single layer of atoms. Reflection high-energy electron diffraction (RHEED) is often used during operation to monitor the growth process. Because of the slow but precise method of MBE, it is a good technique for thin film growth. A typical thickness of GaN grown by the MBE technique is 1-2 μm. A couple of downfalls of the MBE technique are defects in the samples due to particles from surfaces coated during the deposition process falling into the growth beam and contaminating the wafer along with metal

المنارة للاستشارات
www.manaraa.com

contamination.[9] In addition to these issues just mentioned, this is the most expensive method for GaN growth.

1.3 Point Defects

Several factors involved in the growth process of GaN produce point defects and extended defects. These defects hinder the performance of GaN-based devices by affecting their electrical and optical properties. They contribute to excess dark current and noise and reduce the operation lifetime and responsivity of electronic devices. They also reduce the radiative efficiency and operation lifetime of light-emitting devices. The extended defects in a crystal lattice consist of dislocations, clusters, domains, voids and so forth. Although these defects may significantly affect properties of semiconductor devices, they commonly do not contribute to luminescence. Therefore, we will limit consideration to the effects of point defects that can be observed in luminescence experiments. Point defects are native defects, impurities, and complexes that display numerous optical transitions in the luminescence spectra of GaN. [10]

Native defects are formed in semiconductors to compensate for the change in crystal structure due to the introduction of dopants, or as a result nonstoichiometric growth or annealing.[10] The three main forms of isolated native defects are vacancies, interstitials and antisites. A vacancy is an atom that is missing from its atomic site in the crystal lattice. If a neighboring atom fills the vacant site, a vacancy then migrates to the atom's previous location. Interstitial defects are atoms that occupy sites in the crystal lattice that do not normally contain atoms. There are also antisite defects that occur when there is more than one species that makes up the crystal structure and one type of atom occupies another atom's atomic site within that structure.

Another crystallographic defect under consideration occurs naturally because of the impossibility to make any material 100% pure, or purposefully from introduced dopants.

المنارة للاستشارات
www.manaraa.com

Impurities occur when atoms that are not typically contained within the structure replace the native atoms at their atomic site or occupy interstitial sites. When two or more point defects influence each other and form an entity that is different from its constituents, they are referred to as complexes. For example, if an impurity is too large for its site in the lattice structure and it encounters an impurity or a vacancy, the two may bind together. Another complex situation could be two interstitials sharing one atomic site. The concentrations of these point defects can be estimated from their probability of occurrence within the growth process.

The energy needed to create a defect is called the formation energy (E^f) and a defect is less likely to form if this energy is higher.[11] The formation energy of a defect or impurity X in charge state q is given as

$$E^f(X^q) = E^{tot}(X^q) - E^{tot}_{bulk} - \sum_i n_i \mu_i + qE_F\,, \qquad (1)$$

where $E^{tot}(X^q)$ is the total energy of a supercell that contains one impurity or defect X in the charge state q and E^{tot}_{bulk} is the total energy of a defect-free supercell. The number of atoms of type i (host atom or impurity atom) that was added or removed from the supercell when the defect or impurity was formed is n_i, and μ_i is the chemical potential of these species. The Fermi level is E_F, which is the electron chemical potential with respect to the valence-band maximum.[10,12] The chemical potentials of Ga and N taken into consideration here for extreme growth or annealing conditions and are dependent on each other ($\mu_{Ga} + \mu_N = \mu_{GaN}$). The charged defects formation energy is dependent on the charge and the Fermi level at the time that the defect was formed during growth or annealing. Positively charged defects increase the Fermi level toward the conduction band and away from the valence band while negatively charged defects decrease it. The charge state of the defect is proportional to this variation, and the

المنارة للاستشارات
www.manaraa.com

intersection of two different charge states determines the ionization level of the defect. The formation energies for the native point defects in GaN that were calculated as a function of the Fermi level are shown in Fig. 1-5 and the transition levels are illustrated in Fig. 1-6.

The concentration c of a defect, impurity or complex is directly related to the formation energy according to the following equation

$$c = N_{sites} N_{config} \exp\left(-\frac{E^f}{kT} \right), \tag{2}$$

where N_{sites} is the concentration of sites in the lattice (per unit volume) where the defect can be incorporated ($N_{sites} \approx 4.4 \times 10^{22} cm^{-3}$ for GaN), k is the Boltzmann's constant, T is the temperature and N_{config} is the number of configurations that the defect can be incorporated in. If symmetry breaking does not occur, then $N_{config} = 1$ for vacancies, antisites and interstitials. If complexes are formed or symmetry breaking occurs it is the number of configurations in which the defect can be incorporated on the same site.[10,11,12]

It is apparent in that the formation energies for antisites are high and they are not expected to be formed in GaN in significant amounts but gallium and nitrogen vacancies play an abundant role with their low formation energy. Vacancies in GaN are multiply charged defects, and the several defect levels that may appear in the energy gap are represented in Fig. 1-7. The concentrations of gallium vacancies are higher in *n*-type than in *p*-type GaN, while nitrogen vacancies are unlikely to occur in *n*-type but are expected to form in *p*-type GaN. The gallium vacancy, V_{Ga}, is an acceptorlike defect with multiple transition levels and acts as a compensating center. The transition levels of 2-/3-, -/2-, and 0/- are predicted to be 1.10, 0.64, and 0.25 eV from the valence band maximum.[10] These vacancies are mobile in the range of temperatures that are commonly used in growth or annealing processes, making it likely that they migrate and form

المنارة للاستشارات
www.manaraa.com

complexes with positively charged donors.[10,11,12] Theoretically, the variety of transitions in the yellow and green spectrum of photoluminescence (PL) can be attributed to gallium vacancies. Unlike gallium vacancies, the formation energy of nitrogen vacancies, V_N, increases with the Fermi level which makes them more prevalent in *p*-type material.[11] V_N acts like a donor and has only one transition level in the band gap of 3+/+ located at approximately 0.5±0.2 eV above the valence band maximum.[10] Similar to the case of V_{Ga}, V_N is also mobile in the high temperature ranges used for growth and annealing and tend to form complexes with more stable defects.

The formation energy of interstitial defects is high and there is a low probability of them forming. This is a result of a large size difference between Ga and N atoms and a small lattice constant in GaN. The gallium atom has a large size and the formation of gallium interstitials, Ga_i is unlikely in *n*-type material but may form under electron irradiation in GaN or under *p*-type growth conditions. Ga_i is expected to be a donor with a resonance +/- state in the conduction band and a deep 3+/+ state that is predicted to be approximately 2.5 eV above the valence band. This interstitial has high mobility even at room temperatures which leads to the conclusion that Ga_i does not exist in GaN as an isolated defect but rather form complexes after being trapped by some other defect(s). The nitrogen interstitial (N_i) also has a high formation energy that prevents its appearance in GaN grown under equilibrium Ga-rich conditions. It forms a N-N bond where two N atoms share one N site and acts like a simple acceptor. Four stable levels are expected to form in the energy gap due to the different charge states of N_i. The highest of these levels (-/0) occurs at about 2 eV above the valence-band maximum.[10]

Antisite defects, similar to the interstitials, also have a high formation energy and have a low probability of forming in GaN, although, small concentrations may occur under certain conditions. In p-type GaN grown in Ga-rich conditions, gallium antisites (Ga_N) are expected to

www.manaraa.com

introduce a few deep levels and may be responsible for significant compensation and outward lattice relaxation. The Ga_N 4+/3+ level is expected at approximately 0.9 eV above the valence-band maximum. The nitrogen antisite (N_{Ga}) may behave as an acceptor in *n*-type GaN or a compensating double donor in *p*-type GaN. It introduces three to four deep energy levels in the energy gap of GaN, but because of its very high formation energy it is unlikely to form, especially under Ga-rich conditions.[10]

Impurities that are naturally occurring or purposefully introduced in the growth process of GaN act as donors or acceptors depending on the chemical element and its site of occupation. The effect of these impurities on the PL spectrum of GaN has been studied through ion-implantation in response to the search for the most optimum dopant for forming the most efficient luminescence center. The reason for implantation versus vapor introduction was the limit of elements that could be readily introduced during the synthesis of the GaN compound. Other elements must be converted into a volatile compound before they can be used as a dopant.[13] The drawback of using ion-implantation was the damage done to the area of implantation but annealing by a thermal treatment was used to minimize the effect of this damage. The most efficient PL emissions obtained by Pankove and Hutchby were from Zn, Mg, Cd, C, Li, and Si and the spectra of these dopants are displayed in Fig. 1-7. One peak that was observed in all samples studied was a peak at about 1.75 eV, which is attributed to the annealing process, and another peak that was present in all implanted regions was observed at about 2.15 eV. The latter peak was speculated to be implantation related. Two elements that are not only easily introduced in vapor growth of GaN but are also seen as natural contaminates of other elemental species are zinc (Zn) and magnesium (Mg). This paper will focus on these elements along with oxygen (O) and silicon (Si) as impurities and/or dopants involved in the

المنارة للاستشارات
www.manaraa.com

photoluminesence spectra of GaN. Donor energies of Si on a Ga site and O on a N site have been estimated at 30.8 and 32.4 meV, respectively.[10] The formation energies of Si_{Ga} and O_N are small and linearly decrease with the Fermi level, as seen in Fig. 1-8. If these impurities are present in the growth environment there is a high probability that they form in high-resistivity or *p*-type GaN. Acceptor energies of Mg and Zn on a Ga site have been estimated at approximately 220 and 350 meV.[10] Unlike Mg_{Ga}, as seen in Fig. 1-9, and Zn_{Ga} that have low formation energies, the formation energy of the impurity Si_N is relatively high but the formation energies of the acceptors decrease with increasing Fermi level and Si_N formation is expected in undoped or *n*-type doped GaN if Si is present in the growth environment.[10]

The formation energy and concentration calculations presented earlier give a low expectation of simple native defects existing in GaN with substantial concentrations but complexes between native defects and impurities are expected to be the dominant defects that are unintentionally introduced. As previously discussed, vacancies are the dominant native defects expected in GaN. Due to high mobility at temperatures used during growth and annealing, they tend to form complexes with more stable defects. In *n*-type (especially undoped) GaN, the dominant native defect of the gallium vacancy forms stable complexes with donor impurities as a result of the electrostatic attraction between a negatively-charged acceptor and a positively charged donor. The complexes of $V_{Ga}O_N$ and $V_{Ga}Si_{Ga}$ act as double acceptors and are expected to have -/2- energy levels at about 1.1 and 0.9 eV, respectively. The formation of the $V_{Ga}O_N$ complex is more favorable than the formation of V_{Ga} and it is more stable than the $V_{Ga}Si_{Ga}$ complex. This indicates that it may be the dominant compensating acceptor in *n*-type GaN. In *p*-type GaN, the N vacancy is expected to be the dominant and mobile compensating donor that would be attracted to negatively charged acceptors during the growth and annealing processes.

المنارة للاستشارات
www.manaraa.com

The formation energy of a neutral $Mg_{Ga}V_N$ complex is much lower than the sum of the individual formation energies of Mg_{Ga} and V_N but it is unclear where its energy level in the band gap is.[10] To obtain probable concentrations or energy levels of defects and complexes that are created during the growth process, PL spectroscopy is used in evaluation of the optical properties of these defects.

1.4 Photoluminescence from defects in GaN

1.4.1 PL bands in GaN

Identifying defects within semiconductor materials will lead to a better understanding of how they function and will allow the improvement of growth techniques to create high quality devices. There has been a lot of research done to acquire helpful information about GaN and its properties. Photoluminescence (PL) is widely used in the study of GaN because it is very intense and falls into the visible range of the spectrum. The luminescence spectra obtained from this process shed light on the type of defects formed along with their contribution to the functionality of the semiconductor material that is grown with different processes. It also gives us a better view of what types of doping are beneficial, including the increase in the quantum efficiency of emission from the material.

PL is a process in which a substance absorbs a photon; the energy of this photon excites an electron from a lower energy level to a higher energy level, and the subsequent transition of the electron to the lower state produces an emission of a photon with a specific energy. In semiconductors, the incident light excites electrons from the valance band or acceptor levels to either the conduction band or various donor levels, leaving positively charged holes in the valance band. Above-band gap excitation causes the transition of electrons from the valence

المنارة للاستشارات
www.manaraa.com

band to the conduction band and creates a pair of an electron and a hole. Within a matter of nanoseconds the electrons recombine with the holes or are captured by defects. This recombination of the electrons and holes produces photons with energy equal or smaller than the band gap. The spectra obtained from the varying photon energy gives us insight into the properties and defects contained within the crystal structure of the material. Below, the main defect-related PL bands in GaN are briefly reviewed. Fig. 1-10 shows the variety of main bands in PL spectra taken from undoped GaN samples at 15 K.[10]

A broad yellow luminescence (YL) band with a maximum at approximately 2.2 eV is commonly observed in low temperature PL spectra taken from undoped GaN samples. This band is also seen at room temperature from unintentionally and intentionally doped *n*-type GaN samples grown with various techniques along with a near-band-edge emission at about 3.42 eV that is attributed to exciton recombination. Despite the extensive study of the YL band, it is still unclear what the origin of this band is and how doping affects its intensity. The results found in the literature are contradictory. It has been established in the early experiments of Pankove and Hutchby[13] that most of the 35 elements implanted in GaN resulted in appearance and enhancement of the YL band, therefore, the band is most likely related to a native defect caused by implantation damage in their samples. One type defect that has been the focus of attention is the gallium vacancy (V_{Ga}). It is expected that V_{Ga} is the dominant acceptor in *n*-type GaN and it is suggested that Ga vacancies formed during the growth process are bound to defect complexes with O impurities. A positron annihilation experiment conducted by J. Oila et al.[14] on GaN grown on sapphire by HVPE also showed a decrease of the concentration of V_{Ga} from almost 10^{20} cm^{-3} to less than 10^{16} cm^{-3} with an increase of GaN layer thickness from 1 to more than 100 μm. In earlier studies of the YL band, the intensity was considered to be dependent on growth

المنارة للاستشارات
www.manaraa.com

conditions as a result of a rapid reduction of the YL band that was observed as the growth temperature was increased. In contrast, an increase in YL band was observed when GaN was doped with carbon, which indicated that C may be a defect or part of a complex responsible for the YL band. This band has been attributed to the transition from a shallow donor to a deep acceptor and the acceptor was thought to be C or a complex involving C.[10,15,16,17] It was later considered, after doping GaN with C, that C could introduce a defect such as $V_{Ga}C_{Ga}$ that was contributing to the YL band.[15] The only solid assumption that was made from the study was that at least in some GaN samples the YL band originates from a complex consisting of a V_{Ga} and some impurity. The main candidate for the defect responsible for the YL band in undoped GaN is $V_{Ga}O_N$.[10] It may have nearly the same properties as $V_{Ga}C_{Ga}$, since C_{Ga} and O_N are shallow donors but the probability of the formation of C_{Ga} is low. Amidst the controversy in publications, it is well established that the YL band in all GaN samples is related to a transition from the conduction band or a shallow donor to a deep acceptor with ionization energy of approximately 0.8 – 0.9 eV.[10]

The YL band converts into a green luminescence (GL) band for very thick GaN grown by HVPE method; usually these are high-purity GaN samples. The shape and position of a broad yellow-green band depends on excitation intensity and energy and can by deconvolved into two bands. These bands are the YL band that peaks at about 2.22 eV and the GL band that peaks at about 2.48 eV. The GL band is considered to be the result of another charge state of the defect or defects responsible for the YL band.[10]

Another characteristic PL band that is observed in the spectra of undoped GaN at low temperatures is an ultraviolet luminescence (UVL) band. At temperatures below 50K it is referred to as the shallow donor-acceptor pair (DAP) band that has a sharp peak around 3.25 –

المنارة للاستشارات
www.manaraa.com

3.27 eV followed by a number of LO phonon replicas.[18] It is called the DAP band because it is caused by transitions of electrons from the shallow donors to the shallow acceptors. The ionization energy for the shallow acceptors experimentally obtained from GaN layers grown by MBE on sapphire is 170 meV, which is almost identical to previously reported for the UVL band in undoped GaN grown by MOCVD.[19] The ionization energy for the shallow donor is approximately 32 meV. The candidates for the shallow donors in GaN are Si_{Ga} and O_N but there is controversy over the shallow acceptor responsible for the UVL band in undoped GaN. This DAP-type of transition changes to a transition of electrons directly from the conduction band to the same shallow acceptor level as temperature is elevated; and the latter is called the e-A transition. This occurs because, at elevated temperatures (above 50K), the free electrons from the shallow donor are thermally excited into the conduction band. As temperature continues to increase, the UVL band related to the e-A transition broadens and is quenched at temperatures above 120K. Although delineation of the DAP and e-A bands is a challenge, the use of in depth PL studies that include variation of temperature and excitation intensity, along with the use of time-resolved PL, would help to accomplish this.[10]

Another dominant PL band that receives a significant attention of researchers is the blue luminescence (BL) that peaks at about 2.8 - 2.9 eV and is observed with very similar shape and position in undoped, Mg-doped and Zn-doped GaN. The BL band in Mg-doped GaN is attributed to transitions from a deep donor related to a V_N complex to the shallow acceptor Mg_{Ga}[21,22], whereas the BL band in Zn-doped GaN is attributed to transitions form the conduction band or shallow donors to the Zn_{Ga} acceptor.[28] For undoped and Si-doped GaN, the BL band is due to transitions from the conduction band or a shallow donor to an acceptor with ionization energy of 0.34-0.40 eV. The BL band has a fine structure in unintentionally doped GaN when observed at

www.manaraa.com

low temperatures. This structure has sharp peaks associated with local and lattice phonons and is identical amongst different samples. The sharp peaks are separated by an energy of 36±1 meV and then they are repeated at the energies of the LO phonon (91 meV). This fine structure allows analysis of vibrational characteristic of the defect in its ground state.[10] For undoped GaN, the Zn-related BL band is observed only in MOCVD and HVPE grown samples but is never seen in GaN grown by MBE. The most plausible defect responsible for BL band in undoped GaN is Zn_{Ga} that appears as contamination of the sample from impure gases or intentional doping used in the buffer layer for MOCVD and HVPE growths.[10]

A red luminescence (RL) band is observed in undoped GaN grown by HVPE or MOCVD methods that peaks around 1.8 eV and often seen as a shoulder to the YL band. The RL band is less common in the spectra of undoped GaN and is, therefore, less studied than the more steadily observed YL, BL, and UVL bands. The red band can be observed if the YL band is sufficiently weak and can only be resolved at very low excitation intensities. The RL band saturates at very low intensities, and its effective lifetime is the longest amongst other defect-related PL bands of the visible spectrum.[10] There was no energy shift of the RL band detected with delay in time, and it is attributed to the transitions of a shallow donor to a deep acceptor at low temperatures or, at elevated temperatures, from the conduction band to the same acceptor.[22] The acceptor level has a deep energy position of around 1.2-1.3 eV above the valance band which explains its independence from temperature. It is proposed that if a V_{Ga} is trapped by different kinds of extended defects, then an emission similar to the YL band is created but shifted into the red part of the spectrum.[10]

There are two additional peaks that can be observed, near the YL band, in highly resistive samples of GaN. One is a red band that peaks at about 1.8-1.9 eV and the other is a green band

المنارة للاستشارات

www.manaraa.com

peaking around 2.35 eV. These bands are labeled as RL2 and GL2 to distinguish them from the previously discussed RL and GL bands. In a study of 50 GaN samples grown by MBE in Ga-rich conditions and deposited on various substrates, the energy position, shape, and properties were reproduced despite the variation at relative intensity from sample to sample.[10] This observation suggests that bulk type point defects that are almost uniformly distributed are responsible for these bands.

1.4.2 Effects of Temperature in GaN

Temperature also plays a factor in the characteristics of the PL spectra. This has been observed and become an area of focus for over 40 years. It can be seen as a shift of the peak position or variation in line shape of the PL bands depending on temperature and can provide useful information on the type of defects and their nature of transitions within semiconductor materials. Thermal quenching of luminescence peaks is also observed and gives additional information about the properties that are contributing to these peaks. Recombination statistics of PL are utilized to interpret this effect. To explain this temperature dependence, an *n*-type semiconductor containing several radiative acceptors A_i with concentrations of N_{A_i} is taken into consideration. Electron-hole pairs are created in a semiconductor with laser excitation at a generation rate of G [cm^{-3}s^{-1}]. [10] The photogenerated holes from the valence band are created with a total concentration of p. Holes are then captured by acceptors after optical excitation at the rate of $C_{pi}N_{A_i}^{-}p$, where C_{pi} is the hole-capture coefficient for the ith acceptor and $N_{A_i}^{-}$ is the concentration of ionized acceptors of type i. A portion of the recombination of these holes from the acceptor levels with electrons from the conduction band is radiative and observed in the visible spectrum of PL but not all recombination processes are radiative. There are also nonradiative recombination processes that are introduced, for simplicity purposes, as occurring at

المنارة للاستشارات
www.manaraa.com

a rate of $C_{pS}N_S^- p$ where C_{pS} and N_S^- are the average hole-capture coefficient and the concentration of the nonradiative centers.

The holes that are bound to the acceptor level may return to the valence band at elevated temperatures as a result of thermal activation. The probability of this process, Q_i, occurring is proportional to $\exp(-E_i / kT)$, where E_i is the thermal activation energy for the radiative acceptors (E_{A_i}) or nonradiative centers N_S. The detailed balance of this probability of thermal activation of holes is given as

$$Q_{A_i} = C_{pi} g^{-1} N_V \exp\left(\frac{-E_{A_i}}{kT}\right) \tag{3}$$

with

$$N_V = 2\left(\frac{m_h kT}{2\pi\hbar^2}\right)^{3/2} \tag{4}$$

and

$$C_{pi} = \sigma_{pi} v_p = \sigma_{pi}\sqrt{\frac{8kT}{\pi m_h}} \tag{5}$$

where g is the degeneracy factor of the acceptor level, N_V is the density of states in the valence band, m_h is the effective mass of the holes in the valence band, v_p is the hole thermal velocity, and σ_{pi} is the hole-capture cross section of the ith acceptor. [10] The quenching of PL that results from the temperature dependence of N_V and C_{pi} for a recombination channel also affects the integrated PL for other recombination channels at certain temperatures. This causes several increases of the PL intensity in the form of intensity steps that are correlated to the thermal quenching of other PL bands. When one PL band of a particular recombination channel is quenched, the release of holes from this channel is redistributed amongst the unquenched channel and results in a stepwise increase in PL intensity of them.

المنارة للاستشارات

www.manaraa.com

The balance of hole concentration in valence band takes these processes into consideration and can be written for the case of N recombination channels as

$$\frac{\partial p}{\partial t} = G - \sum_{i=1}^{N} C_i N_i^- p + \sum_{i=1}^{N} Q_i N_i^0 = 0 \tag{6}$$

where $N_i^0 = N_{A_i}^0$ and N_S^0 are the concentration of holes bound to radiative acceptors and nonradiative centers, respectively. Since the capture rates are usually much faster than recombination rates, the efficiency of each recombination channel is proportional to *the rate of capture of the minority carriers*. In *n*-type GaN the minority carriers are holes and at low temperatures, where thermal activation is negligible, the internal quantum efficiency (QE) of each recombination channel, $\eta_i(0)$, is given as the ratio of the hole-capture rate of a particular recombination channel to the total escape rate of holes from the valence band. [10] This is given as

$$\eta_i(0) = \frac{C_i N_i p}{\sum_{j=1}^{N} C_j N_j p} = \frac{C_i N_i}{\sum_{j=1}^{N} C_j N_j}. \tag{7}$$

The intensity of PL for each defect can be determined from Eq. (7) as

$$I_i^{PL} = \frac{N_i^0}{\tau_{R_i}} = \eta_i G = \frac{\eta_i^*}{1 + (1 - \eta_i^*)\tau_{R_i} Q_i} G, \tag{8}$$

where the parameter τ_{R_i} characterizes the recombination lifetime, and η_i is the QE of the *i*th channel. It can be found using low temperature QE with the following equation of

$$\eta_i^* = \eta_i(0) \left[1 - \sum_{j \neq i}^{N} \frac{\eta_j(0) \tau_{R_j} Q_j}{1 + \tau_{R_j} Q_j} \right]^{-1}. \tag{9}$$

The temperature dependence of PL intensity that is displayed in QE graphs is used for evaluating the behavior of the luminescence peaks observed in the temperature variant PL spectra of GaN.

المنارة للاستشارات
www.manaraa.com

A brief description of temperature dependence is given below for each of the most dominant and extensively studied PL bands.

Several studies have been done on the topic of the effect of temperature and the shape position and intensity of the YL. In the GaN samples with high QE, a fast decrease of the exciton band intensity is observed at temperatures from 15 to 60 K, which results in a corresponding increase in the defect-related PL intensities, as theoretical representation of this is seen in Fig. 1-11. In the temperature range of 200-260 K, the BL band is quenched and there is, consequently, an increase in the intensity of the YL band. This increase is a result of the redistribution of holes released to the valence band. There have also been reports on the effect of temperature on YL intensity at temperatures above 450-480 K. There is a drastic quenching of the YL at these very high temperatures and the reported values for the activation energy of this process vary from 58 meV to 1040 meV.[24] The activation energies close to 1 eV can be explained by ionization of an acceptor with the activation energy of about 0.85±0.2 eV.[15] The variation of the shape and position of the PL band with temperature has also been the topic of consideration for several publications but there are some discrepancies in the literature. Valuable information can be acquired from studying the effect of temperature on the YL band. The variation of intensity in a wide temperature range, along with thermal quenching, is helpful in estimating the hole-capture coefficient C_p and the hole-capture cross section σ_p for the acceptor responsible for this band. The parameters of C_p and σ_p have been estimated as $(3.3\pm1.6)\times10^{-7}$ cm^3s^{-1} and $(2.7\pm1.3)\times10^{-14}$ cm^2, respectively. Because this capture cross section is so large, it is probable that the acceptor is multiply charged, causing it to be very efficient in capturing holes.[19]

Another band of extensive study is the BL band. The BL band in undoped GaN is thermally quenched at temperatures above 200 K with activation energy of about 340-380

المنارة للاستشارات
www.manaraa.com

meV.[10] This quenching varies with Zn-doped samples that have sample-dependent activation energy. Some samples have rapid quenching that starts above 100 K and other samples maintain high intensity of the BL band up to room temperature. At lower temperatures, the BL band in Zn-doped GaN peaks around 2.87 eV, and is the most easily accessible and dominant band for detailed studies of emission properties since it can be studied without the overlap of other emissions.[25] The rapid quenching of this band has been attributed to sudden redirection of recombination current from radiative to nonradiative recombination.[28]

Another commonly seen and, therefore, studied band is the UVL band. The UVL band in Mg-doped GaN begins quenching at relatively low temperatures and becomes a structureless band at about 3.2 eV with reduced intensity or disappears under the tail of the BL band as room temperature is reached. It has been proposed that this band involves the transition from a shallow donor to a shallow acceptor but the blue-shift of this transition is a result of a small amount of donors along with a high concentration of acceptors, and the transition changes to a recombination of a free electron from the conduction band to the shallow acceptor.[26] The activation energy of this quenching is about 200 meV, which is similar to the reported values obtained in undoped or lightly doped *n*-type GaN.[10,27] The UVL band quenches in a similar fashion for both *n*-type and *p*-type GaN samples. This may be attributed to the abundance of holes at a shallow Mg_{Ga} acceptor site at any temperature, and the small fraction of bound holes that thermally escape would not effect the PL up to room temperature. [10]

1.4.3 Effects of Excitation in GaN

Along with temperature dependence, excitation intensity is also an observed factor that effects the intensity of PL. Saturation of defect-related PL can occur at moderate to high levels of excitation power since the defect concentration and lifetime are finite. Considering the situation

المنارة للاستشارات
www.manaraa.com

of a negligible thermalization of holes trapped by the *i*th acceptor, the intensity of PL related to this acceptor in the case of low QE is

$$I_i^{PL} \approx \frac{G}{\frac{G\tau_{R_i}}{N_i} + \frac{1}{\eta_i}}. \qquad (10)$$

The dependence of PL intensity on the generation rate is linear at low-excitation rates, and at high excitation rates it is expected to saturate at the value of $N_i \tau_{R_i}^{-1}$. This complete saturation is not observed for this case and there is a square root dependence instead for defects in GaN at excitation densities above the range of 10^{-2} W/cm^2. The reason for this square-root dependence is the recombination through nonradiative donors that may have relatively high concentrations in GaN or, perhaps, reabsorbtion of UV emission by deep-level defects.[10,19] Acceptor concentrations in GaN can be determined from the information obtained from the dependence of PL excitation on excitation intensity. The acceptor concentration can also be estimated from PL data by the using Eq. (10). The concentration of the acceptor responsible for the YL band was found by fitting Eq. (10) to experimental data and was estimated to be in the mid-10^{15} cm^{-3} for GaN layers grown by MOCVD.[19] There have been reports of a small shift of the YL band with excitation intensity that indicate that the donor is shallow.[15] The BL band in Mg-doped GaN has shifts of as high as about 0.2 eV that have been reported where excitation intensity was changed by several orders of magnitude, as seen in Fig. 1- 12. Although there is an agreement between researchers investigating the effect of the excitation intensity on the BL band who attribute the band to transitions from a deep donor to the shallow Mg_{Ga} acceptor, there is no consensus about the assignment of the large shift observed. In Mg-doped GaN, the UVL band was found to blueshift with increasing excitation intensity and, in some GaN:Mg samples, the band appeared as a structureless broad band peaking at about 3.1-3.2 eV. An interesting observation, which has

المنارة للاستشارات
www.manaraa.com

long been reported and still remains unexplained it that the intensity of the BL band increases linearly with excitation intensity but the increase of the UVL band with intensity was quadratic.[10]

المنارة للاستشارات
www.manaraa.com

Chapter 1 Figures

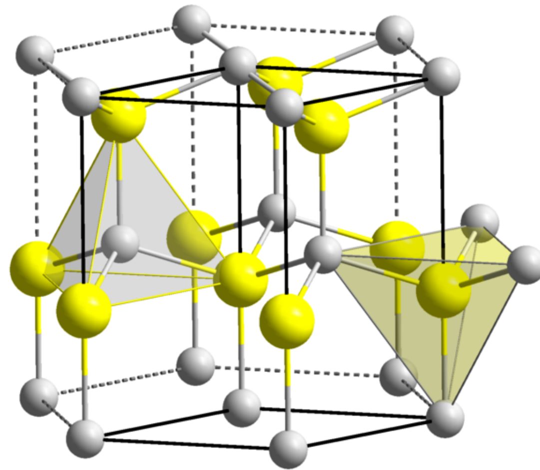

Fig. 1-1: Wurtzite crystal structure of GaN. The larger yellow atoms are Ga and the smaller white atoms are N. (http://en.wikipedia.org/wiki/File:Wurtzite_polyhedra.png)

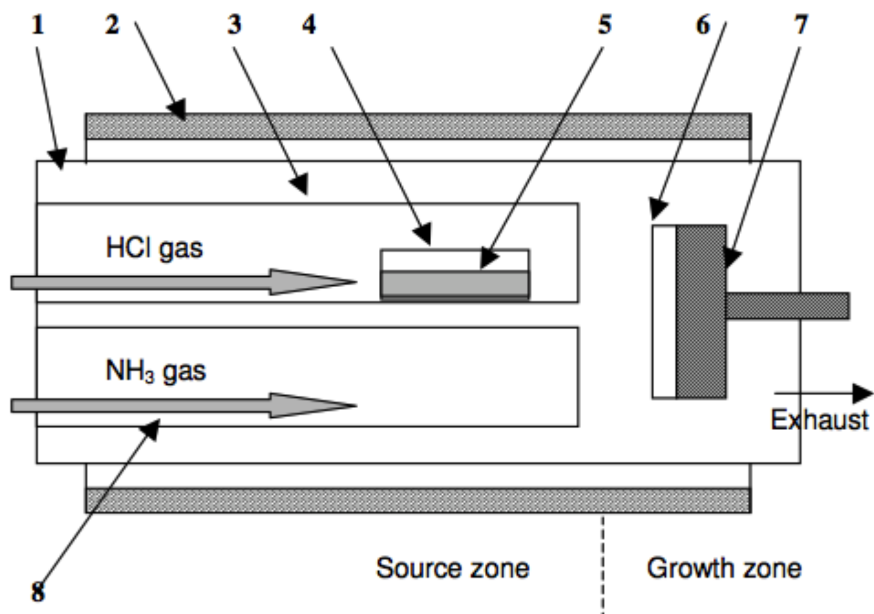

Fig. 1-2: Schematic illustration for GaN HVPE growth: 1 – main reactor tube, 2 – heating elements, 3 – Ga source gas channel, 4 – boat with Ga Melt, 5 – Ga melt, 6 – substrate, 7 – substrate holder, and 8 – ammonia source tube.
(www.oxford-instruments.com/products/etching.../hvpe.aspx)

المنارة للاستشارات
www.manaraa.com

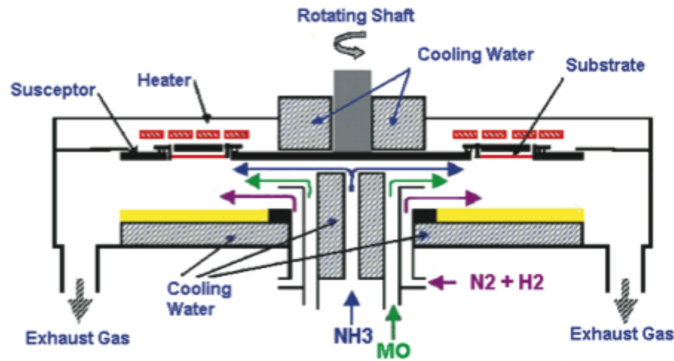

Fig. 1- 3: Schematic illustration for MOVPE growth. Face-down multiwafer set-up, gear driven rotation, separated flow of active species (courtesy EMC, Japan).

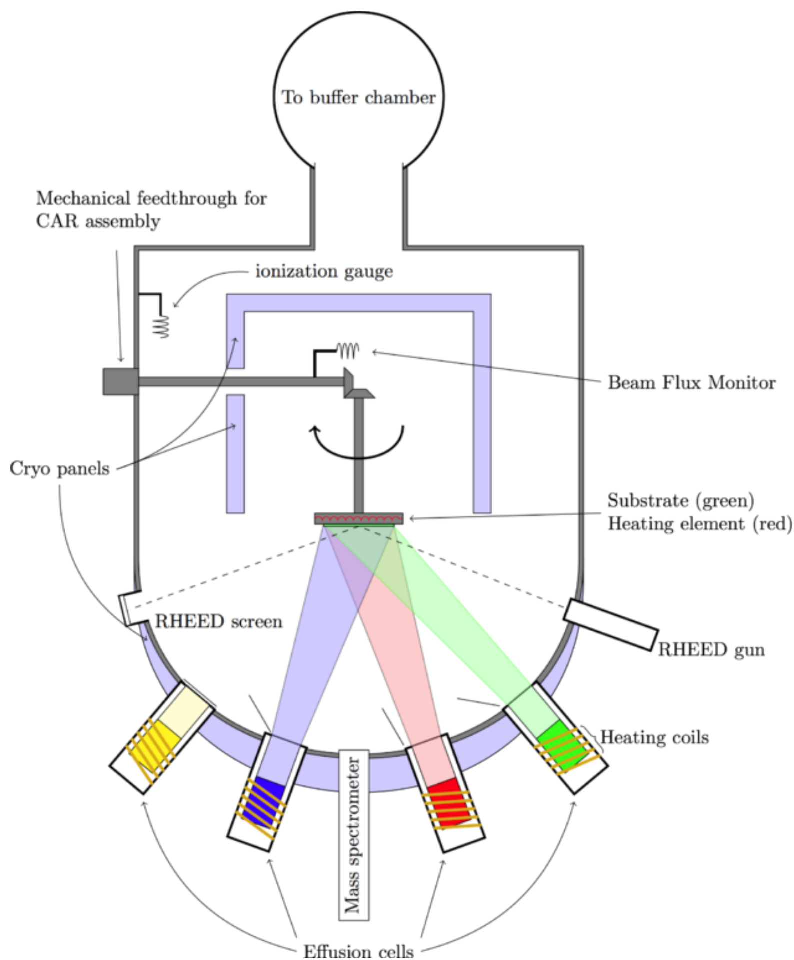

Fig. 1-4: Schematic illustration for MBE growth. A simple sketch that shows the main components, rough layout and concept of the main chamber.
(http://en.wikipedia.org/wiki/File:MBE.png)

المنارة للاستشارات
www.manaraa.com

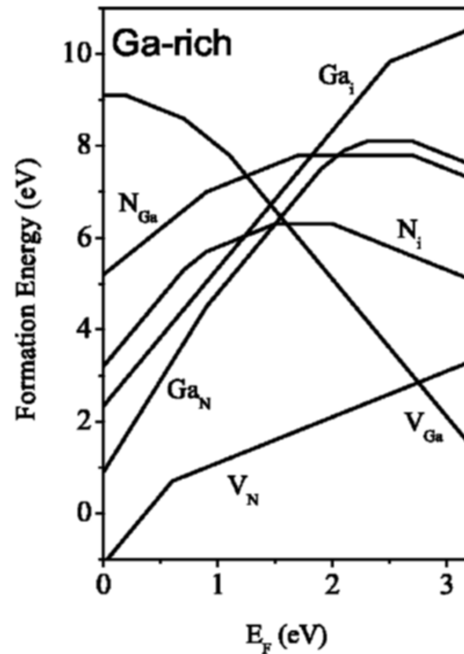

Fig. 1-5: Formation energies for native point defects in GaN as a function of Fermi level. The zero of the Fermi level represents the top of the valence band. Only segments related to the lowest-energy states are shown and their slopes indicate their charge state. The transition between charge states can be seen in the kinks of the curves.[12]

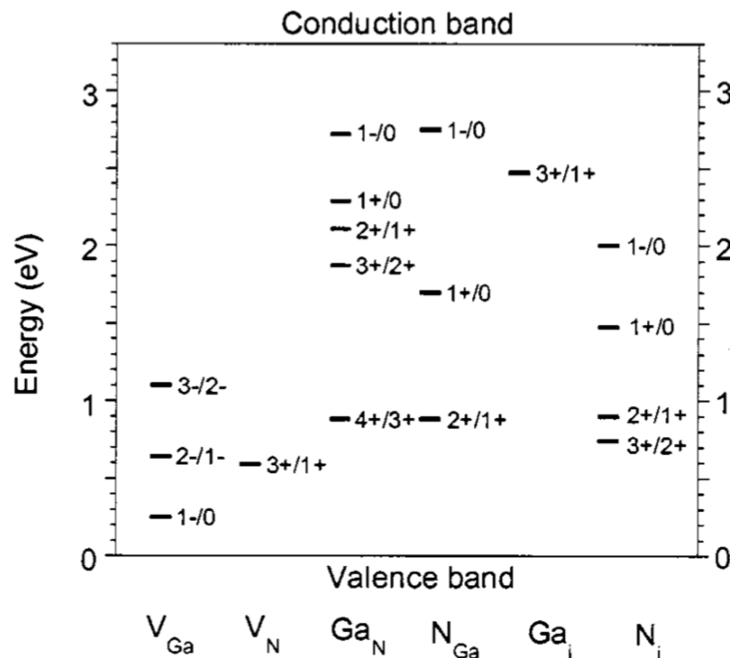

Fig. 1-6: Transition levels that were determined from **Fig. 1-5** for defects in GaN.[10]

www.manaraa.com

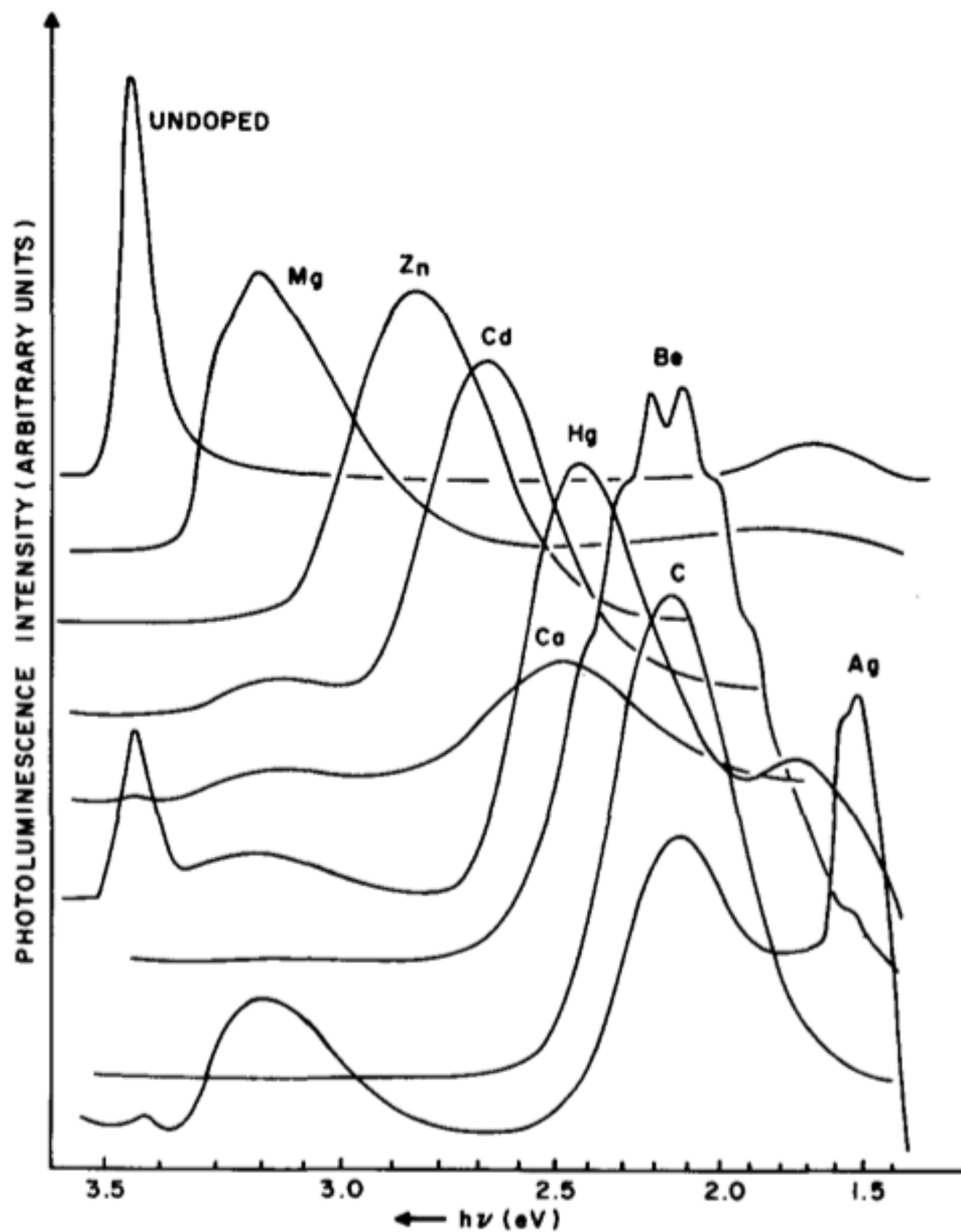

Fig. 1-7: Photoluminescence spectra of undoped GaN of several implanted elements at 78° K.[13]

المنارة للاستشارات
www.manaraa.com

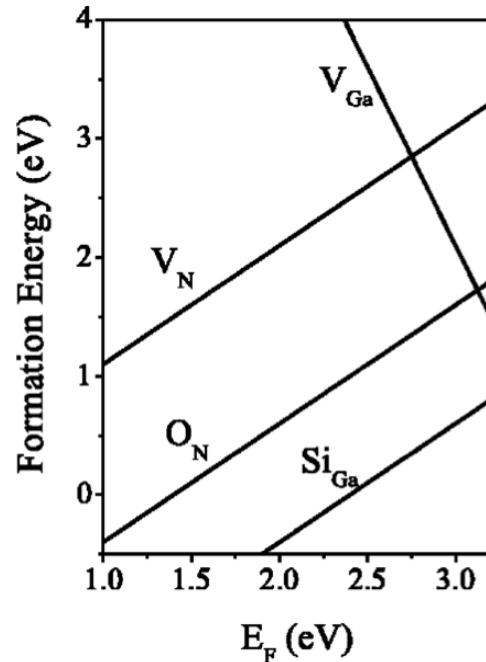

Fig. 1-8: Formation energy as a function of Fermi level for native defects (nitrogen and gallium vacancies) and impurity donors (oxygen and silicon) in GaN in gallium-rich conditions.[12]

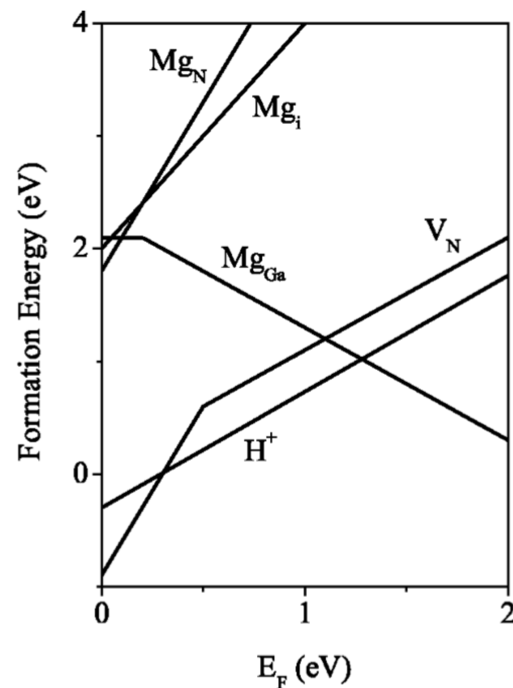

Fig. 1-9: Formation energy as a function of Fermi level for magnesium in different configurations along with the native defect of a nitrogen vacancy and hydrogen interstitial in gallium-rich conditions.[12]

المنارة للاستشارات
www.manaraa.com

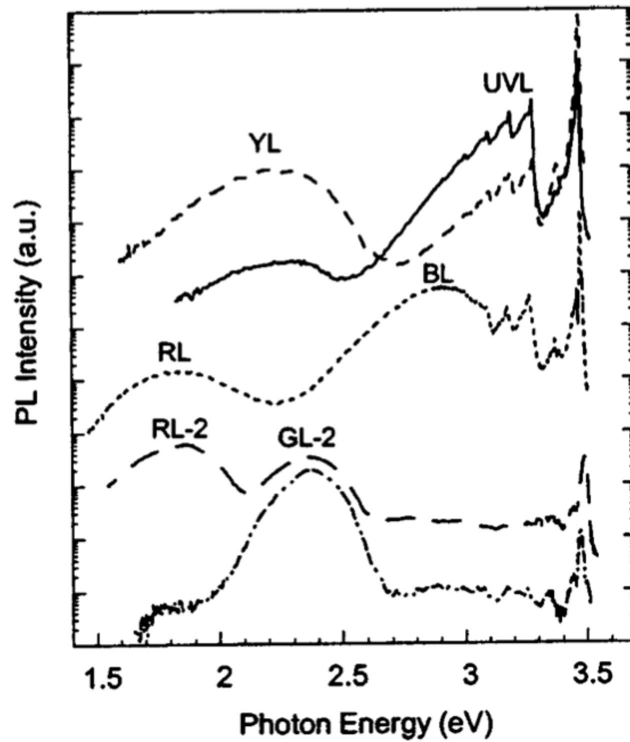

Fig. 1-10: PL spectra from undoped GaN at 15 K. The spectra are plotted in logarithmic scale and displaced vertically for better viewing.[10]

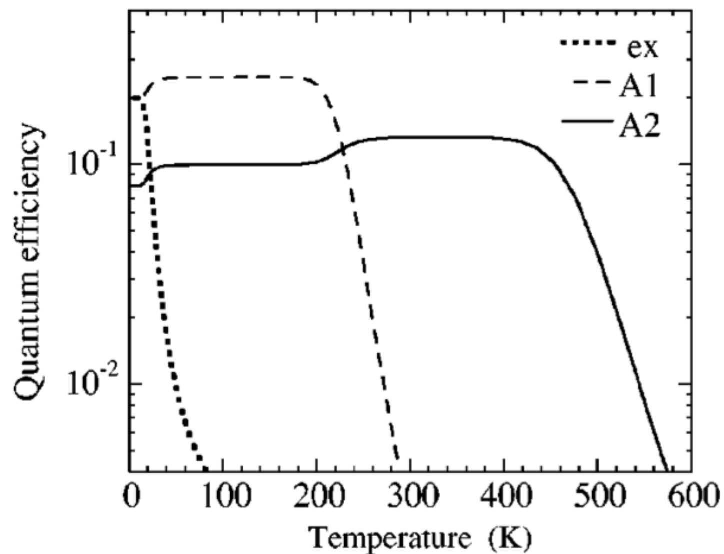

Fig. 1-11: Calculated temperature dependencies of the QE for radiative recombination channels in GaN of excitons and two acceptor channels (A1 and A2).[19]

المنارة للاستشارات

www.manaraa.com

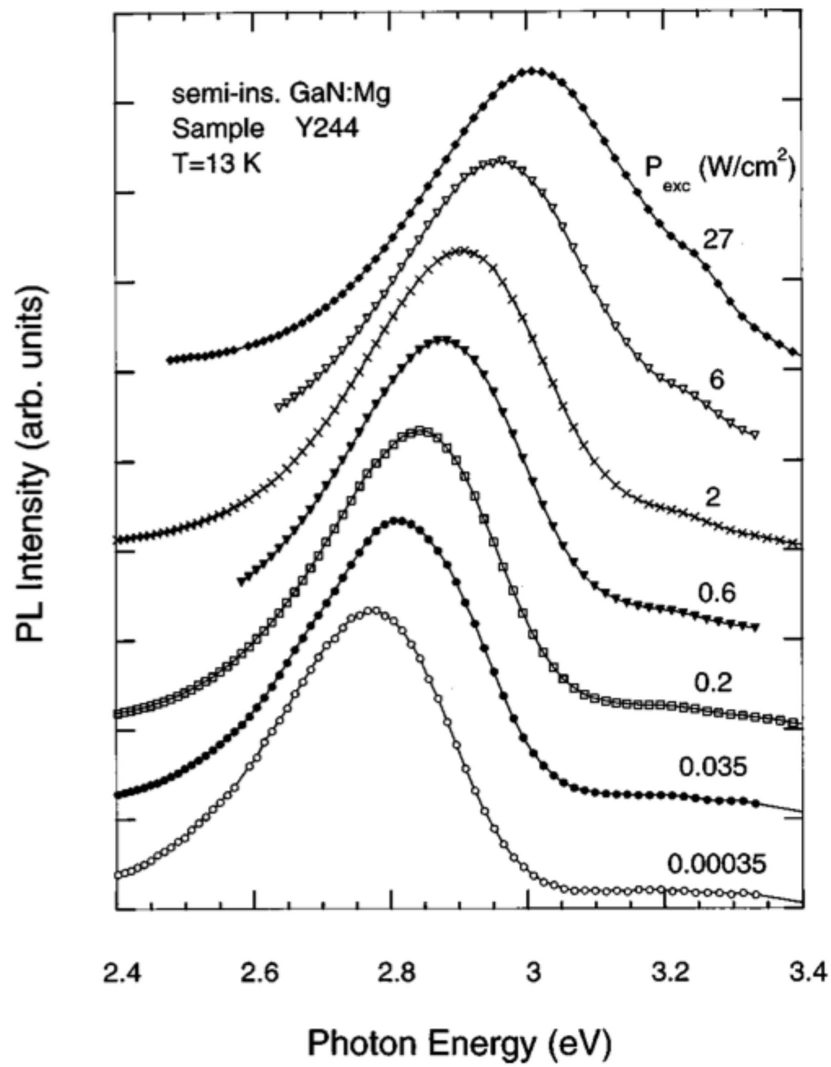

Fig. 1- 12: Low-temperature PL spectra at different excitation intensities of a Mg-doped GaN sample.[26]

المنارة للاستشارات

www.manaraa.com

Chapter 2. Experimental Details

2.1 Sample

The sample that was studied in detail was a Zn-doped GaN layer (sample # ap274) grown at TDI, Inc. using the HVPE method on the *c*-plane sapphire. A thickness of 4.8 μm was estimated based on growth conditions. The atomic concentration of Zn was determined by TDI through measuring by means of SIMS and was uniform through the layer thickness. This concentration was reported by TDI to be $1.7 \times 10^{17} cm^{-3}$. A highly conductive *n*-type layer is sometimes formed in GaN grown by the HVPE method near the GaN/sapphire interface due to contamination with oxygen. This layer prevents the ability to determine the exact resistivity values due to the shunting of the high-resistivity bulk region in electrical measurements. This also hinders the ability to decipher whether the sample is *n*-type or *p*-type.[28]

2.2 Experimental set-up

The necessary components of a PL set-up are a laser as an excitation source, a spectrometer or monochromator to analyze the PL spectrum, a detector to convert an optical signal into an electrical signal and other optical and electronic accessories that filter, focus and direct laser light and PL.

A simplified top view of the set-up used in our lab to obtain measurements of steady-state PL is shown in Fig. 2-1 . The main components are a laser, a cryostat, a monochromator, and a PMT detector. PL is excited with a continuous-wave Helium Cadmium (HeCd) laser with 50 mW of power and photon energy 3.81 eV. The HeCd laser is a gas laser that uses helium in conjunction with cadmium that is vaporized at a relatively low temperature. This IK Series HeCd

المنارة للاستشارات
www.manaraa.com

laser from Kimmon produces a high quality beam at 325 nm. The laser is non-destructive to the samples and emits photons with energy higher than GaN bandgap. It is, therefore, a good choice for use in photoluminescence experiments.

The HeCd laser light is directed through a UV prism and a diaphragm slit to select the 325 nm line and block other emission lines. It is then reflected off of mirrors for convenience of alignment and passed through various neutral-density filters to attenuate the excitation intensity. An excitation power density (P_{exc}) from 2 x 10^{-7} to 0.3 W/cm^2 can be obtained using an unfocused beam with a diameter of 4 mm, and a P_{exc} up to 200 W/cm^2 can be obtained using focused beam with diameter of 0.1-0.2 mm. Variation of power density alters the PL spectra. The resulting beam continues toward a sample that is encompassed in a closed-cycle optical cryostat. The cryostat allows variation of temperature during experimental acquisition.

Since temperature is another variable that greatly affects the PL spectra, the samples were encompassed in a closed-cycle optical cryostat to vary the temperature from 15 to 330 K. A cryostat (cryo = cold and stat = stable) is a vacuum chamber that uses nitrogen or helium gas to drop the temperature to, in our case, 15K. The chamber obtains a high vacuum of up to 10^{-5} Pa with a turbomolecular pump. The sample is sandwiched between a copper holder and a flat sapphire window, with an indium spacer between the sample and the copper plate for better thermal contact. The sample is mounted inside of the cryostat, and light is focused on the center of the sample. The luminescence is then collected with a lens and directed through color filters to collect PL of a certain wavelength range and to eliminate scattered light at 325 nm PL from stronger luminescence peaks into the monochromator. A 560 nm long pass (yellow filter) was used for the range of 560 – 820 nm to suppress strong emission from the UV or blue region.

المنارة للاستشارات
www.manaraa.com

The monochromator is an optical device that transmits a light in a selected narrow band of wavelengths. The word comes from the Greek roots of "mono" which means single, "chromo" which means color and the Latin suffix of "ator" which denotes an agent. The wavelengths are dispersed by the use of a diffraction grating. A typical Czerny-Turner monochromator, a model similar to the one used in our experiments, is shown in Fig. 2-2. A is the beam coming into the slit B. C is a concave mirror that collimates (focuses at infinity) the beam. The collimated light is then refracted by a diffraction grating D and collected by another mirror at E that refocuses the light toward the exit slit F. The separated wavelengths exit through G and are selected by the rotation of the grating. In our experiment, a 1200 rules/mm grating in a 0.3 m monochromator model Triax 300 from Jobin Yvon Horiba is used.

The selected light G, in Fig. 2, is directed into the Photomultiplier Tube (PMT). The PMT used in our experimental set-up was a model R928 from the Hamamatsu Co. This element reduces the temperature to approximately -40° C by using a Peltier element and chilled water to reduce the noise in the PL spectra by at least two orders of magnitude, as seen in Fig. 2- 4. The PMT multiplies the current produced by the exiting light G to enable individual photons to be detected when the flux of light is very low. An example of a PMT can be seen in Fig. 2-3. The photomultiplier tube consists of a cathode, an anode and several grids encompassed in a glass envelope with a high vacuum inside. The incident photon from G strikes the photocathode material (thin deposit of a multialkali substance on entry window) and produces electrons as a consequence of the photoelectric effect. The focusing electrode directs the electrons toward the electron multiplier by the process of secondary emission. The dynodes cascade the electrons to the anode for detection of the incoming photon. An electronic device called a photon counter analyzes the electrical signal from the PMT. Then, the data is fed into a computer and graphed

المنارة للاستشارات
www.manaraa.com

with a program called SynerJy through the electrical connection. The raw data is then transferred to another program called Kaleidagraph where it can be used for different graphical interpretation.

المنارة للاستشارات
www.manaraa.com

Chapter 2 Figures

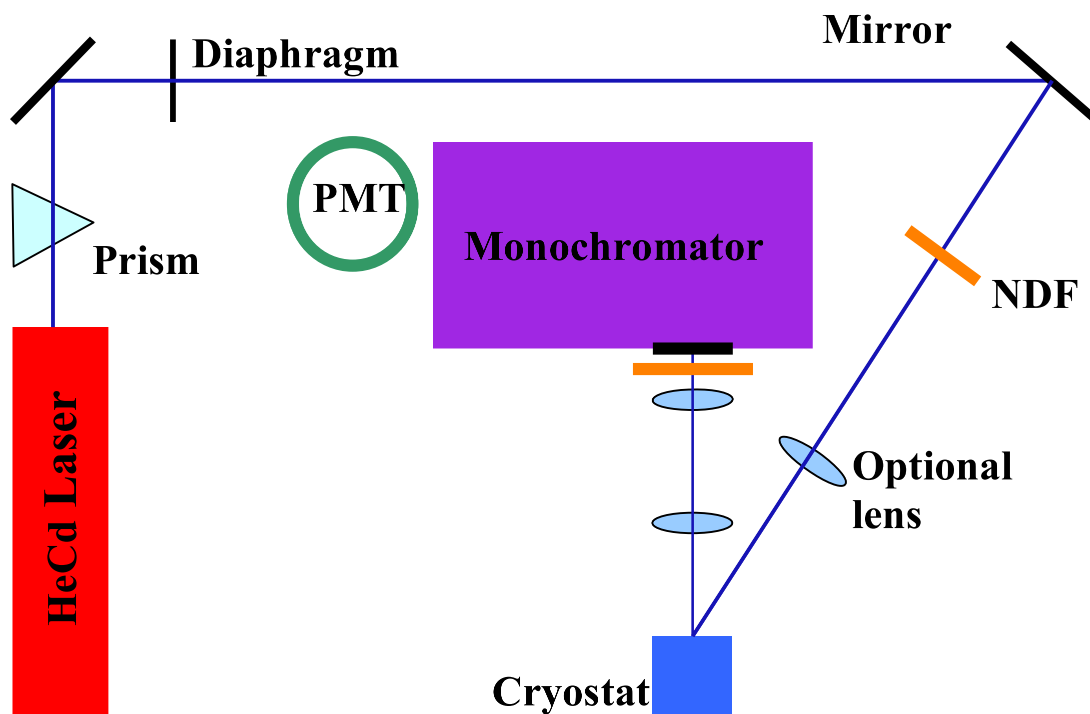

Fig. 2-1: Simplified view of experimental set-up for photoluminescence experiments.

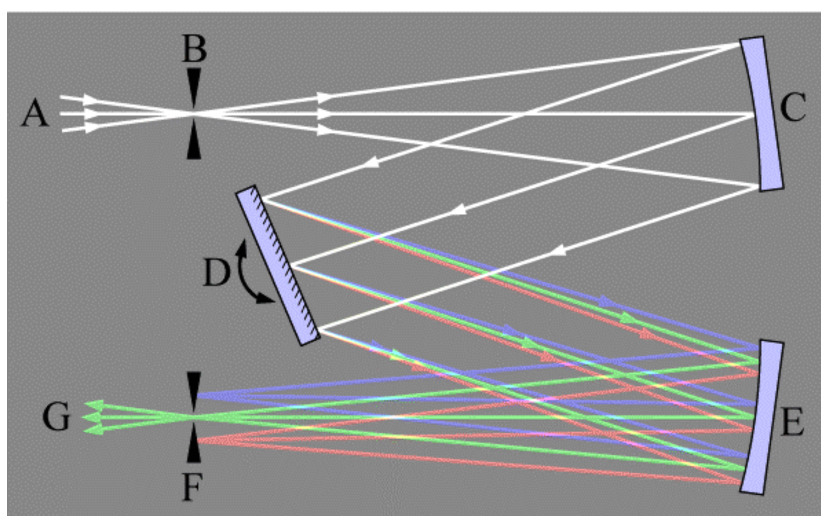

Fig. 2-2: Diagram of a Czerny-Turner monochromator.
(http://en.wikipedia.org/wiki/File:Czerny-turner.png)

www.manaraa.com

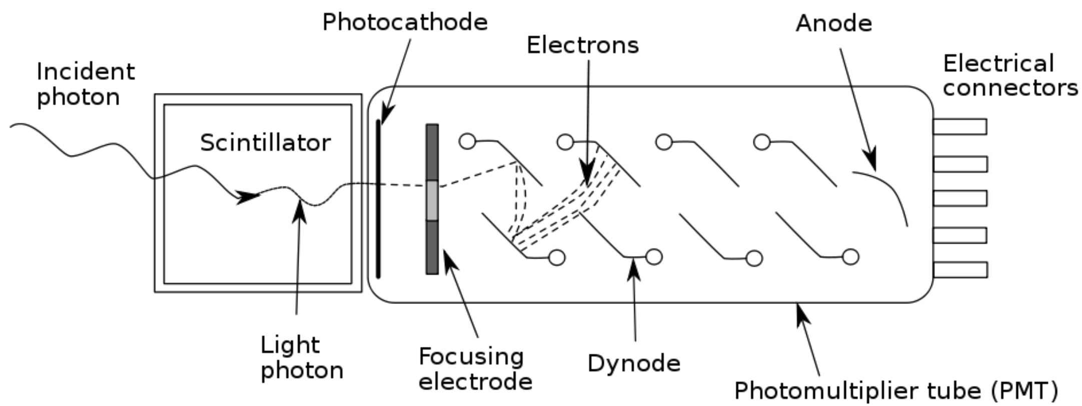

Fig. 2-3: Schematic of a photomultiplier tube (PMT)
(http://en.wikipedia.org/wiki/File:Photomultipliertube.svg)

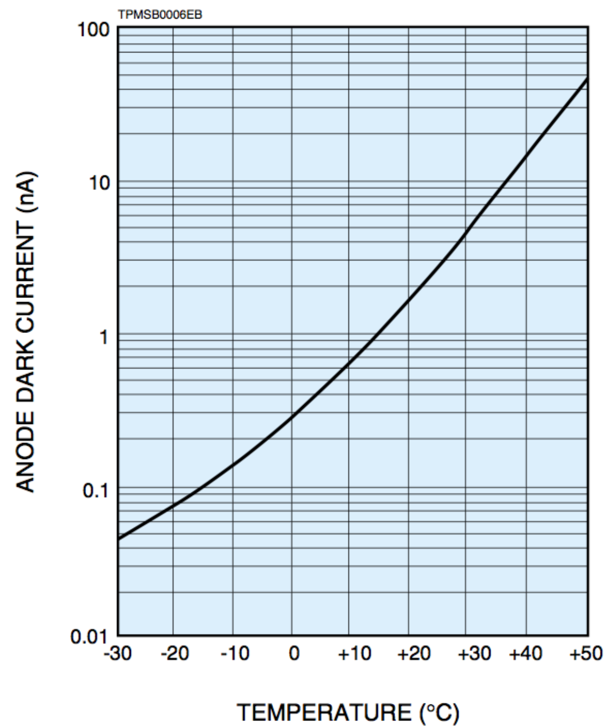

Fig. 2- 4: Typical temperature characteristics of Dark Current at 1000 V, after 30 min storage in darkness. (www.hamamatsu.com)

المنارة للاستشارات
www.manaraa.com

Chapter 3. Experimental Results

3.1 Low Temperature PL Spectra of Zn-doped and undoped GaN

The PL spectra obtained from our Zn-doped GaN sample (ap274) have similar features to that of spectra previously acquired in undoped GaN samples. Fig. 3-1 shows a comparison of these similarities in a low-temperature PL spectra of an undoped sample (th1011) and Zn-doped sample (ap274). For the undoped sample, the spectrum shows an excitonic luminescence (from 3.3 to 3.5 eV) that has a sharp and intense line at 3.47 eV and a weaker peak at 3.455 eV; an ultraviolet luminescence (UVL) band (from 3.1 to 3.3 eV) with a main peak at 3.26 eV and an LO phonon replica; and a blue luminescence (BL) band (from 2.2 to 3.1 eV) that peaks at 2.9 eV. This spectrum is tailed by a structureless red luminescence (RL) band (from 1.5 to 2.2 eV) with a maximum at 1.8 eV but is not shown in Fig. 3-1.[28] For the distinct peaks in the excitonic luminescence spectrum, the most intense line is attributed to the exciton bound to a neutral shallow donor and the weaker peak at 3.455 eV is attributed to the exciton bound to the neutral Zn_{Ga} acceptor. There is a characteristic structure seen in the BL band that includes a zero phonon line at 3.085 eV and other peaks that are associated with two phonon modes, which are an LO mode with phonon energy of 91 meV and a local or pseudolocal mode with phonon energy of 36 meV. [28]

The Zn-doped GaN sample (ap274) has a spectrum consisting of an excitonic luminescence (from 3.3 to 3.5 eV) with an intense peak at 3.45 eV and a weaker peak at 3.46 eV and both are followed by LO phonon replicas; a UVL band (from 3.1 to 3.3 eV) with the main peak at 3.26 eV and a LO phonon replica; and a BL band (from 2.2 to 3.1 eV with a peak at 2.9 eV. The PL spectrum we obtained from ap274 is also tailed by a structureless red luminescence band (from 1.5 to 2.1 eV) with a maximum at 1.8 eV, this is seen in Fig. 3-2.The fine structure of

www.manaraa.com

the BL band is observed in its high-energy part, and it allows us to identify, with certainty, the defect responsible for the PL band. The BL band in both undoped and Zn-doped GaN is attributed to the transition from a shallow donor (at low temperatures) or from the conduction band (at elevated temperatures) to the Zn_{Ga} acceptor. [28] In undoped GaN, the presence of Zn is due to uncontrolled contamination during the growth process. Because there is a fairly distinct assignment to acceptor responsible for this band, special attention is paid to this band.

3.2 The effect of Temperature on PL Intensity

We observed a dramatic drop in the PL intensity of the BL band in the Zn-doped GaN (ap274) PL spectra as temperature was increased from 13 to over 300 K. In order to appreciate the unusually abrupt drop in PL intensity that is observed in this Zn-doped sample, a comparison of PL data for this sample and an undoped GaN sample is presented in Fig. 3-3.This figure shows the thermal quenching of the BL band that takes place with increasing temperatures of the two samples, and it is apparent that the Zn-doped sample has a much more abrupt thermal quenching than the undoped GaN sample. The activation energy of the quenching, that can be determined from the slope of dependence in the Arrhenius plot, is about 0.35 and 1.0 eV for the undoped and the Zn-doped GaN samples, respectively.

Fig. 3-4 shows the evolution of the PL spectrum with increasing temperature for the Zn-doped (AP274) sample obtained at P_{exc} = 0.3 W/cm^2. The excitonic luminescence (see Fig. 3-5) has three distinguishable peaks near 3.45 eV at 15 K. A dominant peak in the center with a maximum at 3.45 eV is due to an exciton bound to a Zn_{Ga} acceptor, and a peak with a maximum at 3.46 eV is due to an exciton bound to a shallow donor. A peak at 3.43 eV is a phonon replica (other than LO) of the 3.45 eV line. These three peaks are accompanied by phonon replicas at distances that are multiples of the LO phonon energy (91 meV). As seen in Fig. 3-5, the main

المنارة للاستشارات
www.manaraa.com

excitonic peak of 3.46 eV develops a shoulder, which becomes a peak with a maximum at 3.47 eV at 30 K. This peak is attributed to a free exciton and it dominates the excitonic band above 40 K. It shifts to lower energies due to the shrinkage of the band gap. The free exciton peak dominates after 50 K and replaces the 3.46 eV peak by the temperature of 60 K. There is a rapid decrease of the two other peaks with maxima of 3.43 and 3.45 eV and they are also lost from the spectrum as the temperature of 60 K is reached. These two peaks disappeared because the exciton bound to the Zn_{Ga} acceptor is ionized and becomes a free exciton at a relatively low temperature. The phonon replica also develops an addition peak with a maximum at 3.38 eV that appears at 40 K and dominates by 50K. This is the LO phonon replica of the free exciton peak. The peaks of 3.34 and 3.36 eV are also lost from the spectra by 70 K because they are phonon replicas of the acceptor bound exciton peaks. The remaining replica peak has a very slight redshift (from 3.38 to 3.36 eV) as temperature increases, becomes broad and structureless when it reaches the temperature of 140 K, and becomes indistinguishable by 230 K. The main excitonic luminescence peak also has a slight redshift (from 3.47 to 3.41 eV) in the temperature range of 60 K to 325 K. The excitonic luminescence band is the dominant band in the spectrum for the temperature range of 15-110 K but is overcome in peak height by the BL band in the temperature range of about 110-300 K. It dominates again at temperatures above 310 K as the BL band is thermally quenched. Two peaks, seen at 3.27 and 3.25 eV, are the second LO phonon replica of the Zn_{Ga}-acceptor bound exciton ($3.45 \text{ eV} - 2 \times 91 \text{ meV} \approx 3.27 \text{ eV}$). A peak at ~3.17 eV is most probably the third LO phonon replica. With increasing temperature, the exciton emission quenches first, so that at temperatures above 40 K we can see the UVL band with the main peak at 3.27 eV. In the temperature range between 40 and 130 K, the acceptor bound exciton disappears, but the UVL band slightly decreases.

المنارة للاستشارات
www.manaraa.com

The band of most importance is the BL band because of the extreme thermal quenching observed in this sample. The BL band peaks at 2.87 eV at a temperature of 15 K as seen in Fig. 3-4.The intensity of this band is almost constant in the temperature range from 15 to 130 K, and a slight decrease of intensity occurs at the temperature range of 140 to 190 K. As temperature rises above 190 K, there is a dramatic thermal quenching that is observed in the BL band, and it is completely quenched by 325 K. A gradual broadening of the peak with the increase in temperature from 15 to 190 K and a slight blueshift (from 2.87 to 2.91) over the entire temperature range of 15 to 325 K, were also observed.

At higher excitation intensity, as seen in Fig. 3-7, where P_{exc} = 12.2 W/cm^2, the excitonic luminescence peak remains the dominant peak with increase in temperature up to 110 K. The spectrum obtained at 15 K (see Fig. 3-8) show the same details as those observed at the excitation intensity of 0.3 W/cm^2. There is a main excitonic peak followed by two or three LO phonon replicas. The main excitonic peak consists of three peaks with maxima of 3.43, 3.45, and 3.46 eV, and the first LO phonon replica consists of two peaks with maxima of 3.34 and 3.36 eV. The main excitonic peak follows the same pattern as previously discussed, namely a shoulder peak (at 3.47 eV) which is the free exciton, emerges from the 3.46 eV peak at 30 K and dominates the excitonic luminescence band at higher temperatures. The two other peaks associated with the exciton bound to the Zn_{Ga} acceptor rapidly reduce their intensity and are no longer visible at the temperature rises to 60 K. The remaining free exciton peak continues to be the dominant peak of the excitonic luminescence 60 K and displays a redshift (from 3.47 to 3.39 eV) as temperature in increased to 320 K. The LO phonon replicas repeat this pattern with a peak (at 3.38 eV) emerging at 40 K that becomes the dominant phonon peak by 50 K. The intensity of the two original Zn_{Ga}-related phonon peaks quickly decreases and they are no longer visible by

المنارة للاستشارات
www.manaraa.com

the temperature of 70 K. The intensity of the remaining LO phonon replica of the free exciton peak steadily decreases as temperature is increased, becomes broad and structureless by 250 K and is no longer visible in temperatures above 310 K. It also displays a slight redshift (from 3.38 to 3.36 eV) over the entire temperature range. The intensity of the excitonic luminescence band as a whole decreases quickly in the temperature range of 15 to 40 K but then decreases very slowly and steadily as temperature is increased from that point on. It is difficult to resolve the UVL band at P_{exc} = 12.2 W/cm^2.

The BL band peaks at 2.90 eV (at 15 K, see Fig. 3-7). Its intensity remains nearly constant in the temperature range from 15 to 140 K and then decreases abruptly as temperature increases to 290 K. The rate of thermal quenching of the BL band is the highest in the temperature range of 290 to 320 K but complete thermal quenching was not observed at this excitation intensity with the highest temperature obtained in this experiment.

At a much lower excitation intensity, as seen in Fig. 3-9 where $P_{exc} = 0.00027$ W/cm^2, the excitonic luminescence band at 15 K (see Fig. 3-10) has a main peak at 3.44 eV and a phonon replica peak at 3.35 eV. The PL intensity of this band is significantly lower and it is less defined than the excitonic luminescence band observed at higher excitation intensities because wider slits of the monochromator were used in this experiment. The phonon replica peak at 3.35 eV quickly disappears by the temperature of 40 K, whereas the main peak intensity drops rapidly in the temperature region of 30 to 50 K and then continues to decrease at a much slower rate.

The UVL band is relatively strong at this excitation intensity and, at 15 K (see Fig. 3-10), has a peak with a maximum at 3.25 eV, along with a phonon replica peaking at 3.16 eV. The phonon peak is no longer visible in the spectrum by a temperature of 40 K. The intensity of the UVL band slowly decreases in the temperature range of 15 to 100 K, rapidly quenches from 100

المنارة للاستشارات
www.manaraa.com

to 110 K, and then disappears under other bands rate at higher temperatures. There is slight blueshift (from 3.25 to 3.28 eV) that is observed with increase in temperature.

The BL band, at this excitation intensity, is the dominant peak with increase in temperature until it is thermally quenched. The maximum of the BL band at 15 K (see Fig. 3-9) is at 2.86 eV and its intensity slowly decreases as the temperature is increased to 160 K. The band begins quenching faster at 160 K, and the PL intensity dramatically drops as the temperature is increased up to 210 K. The band continues to quench and disappears under the wing of a higher energy band at temperatures above 260 K and is completely quenched at 280 K. A blueshift (from 2.86 to 2.96 eV) of the peak maximum is observed over the entire temperature range.

Temperature dependence graphs were experimentally obtained from a Zn-doped GaN sample at the three different excitation intensities of 0.3, 12.2 and 0.00027 W/cm^2. Thermal effects, along with thermal quenching, were observed and documented for three PL bands, namely, the excitonic luminescence band, the UVL band and the BL band. The excitonic luminescence and UVL peaks had similar quenching characteristics, and the excitonic structure was especially well defined at higher excitation intensities, but quenched rapidly and had less detailed definition at lower excitation intensities. For the excitonic luminescence band at the excitation intensity of 12.2 W/cm^2, thermal quenching began at a higher temperature than for the spectra taken at 0.3 W/cm^2. The quenching of the BL band occurs at higher temperatures at higher excitation intensities. At an excitation intensity of 12.2 W/cm^2, the BL band does not completely quench within the temperature range of the experiment (from approximately 13 to 320 K) but there is complete thermal quenching of the BL band in the other two excitation intensities under observation. At an excitation intensity of 0.00027 W/cm^2, the thermal

المنارة للاستشارات
www.manaraa.com

quenching of the BL band happens long before the peak experimental temperature is reached but at the excitation intensity of 0.3 W/cm^2, it takes the entire temperature range for the BL band to completely quench. Observing the temperature dependence at three different excitations and seeing the variation in results shows that there is also a dependence on excitation intensity.

3.3 The effect of Excitation on PL Intensity

As shown in the graphs of temperature dependence, the dominance of the BL band in the spectra of Zn-doped sample increases as the excitation intensity is decreased. Fig. 3-11 shows the dependence of PL intensity on excitation intensity at the temperature of 13 K. The excitonic luminescence band consists of a main peak that has three maxima peaks (at 3.43, 3.45 and 3.46 eV) and a phonon replica with two (at 3.34 and 3.36 eV), as seen in Fig. 3-12. The shape and positions of the details in the main peak remain consistent. The normalized PL intensity (PL intensity divided by the excitation intensity) and decrease in intensity at a fairly constant rate as excitation intensity is lowered. The UVL band consists of a main peak at 3.25 eV and a phonon replica, and can be resolved only at $P_{exc} < 0.01$ W/cm^2 (Fig. 3-13). The normalized intensity of the PL of the main peak in the UVL band remains fairly constant as excitation is further decreased. The phonon replica of the main UVL peak has similar behavior and it can be well observed at 3.16 eV peak at at $P_{exc} < 0.01$ W/cm^2. The BL band has an opposite reaction to the change in excitation intensity than that of the excitonic luminescence band. As excitation intensity is decreased the normalized PL intensity of the BL band (along with the RL) increases at a constant rate. This behavior can be explained by partial saturation of the Zn_{Ga} acceptors with photogenerated holes. Fig. 3-14 shows PL spectra at three selected excitation intensities for which the temperature behavior was analyzed in more detail. There is abrupt thermal quenching of the BL band observed at a specific temperature but this value is also dependent on excitation

المنارة للاستشارات
www.manaraa.com

intensity, as seen in Fig. 3-15.The behavior of this tunable quenching can be explained by a rate equation model and theoretically analyzed with mathematical modeling software.

للاستشارات المنارة
www.manaraa.com

Chapter 3 Figures

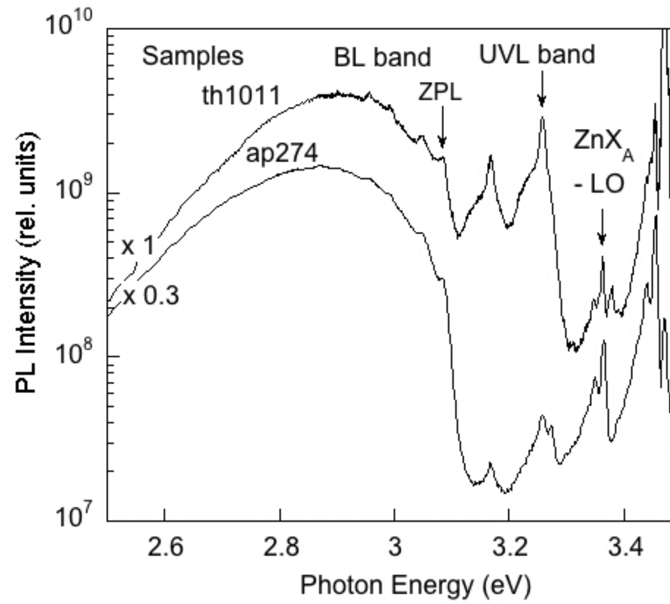

Fig. 3-1: PL Spectra from undoped (sample th1011) and Zn-doped GaN (ap274) at a temperature of 13 K and P_{exc} = 0.002 W/cm^2. The Zn-doped data has been multiplied by 0.3.

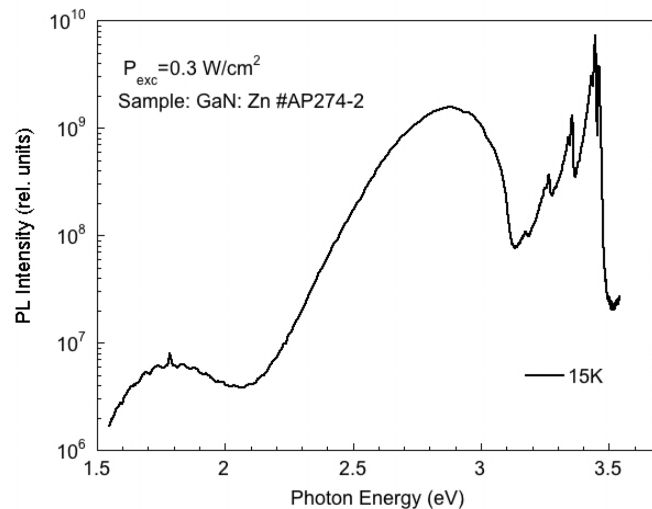

Fig. 3-2: PL Spectra of a Zn-doped GaN (sample ap274) at a temperature of 15 K and P_{exp} = 0.3 W/cm^2.

المنارة للاستشارات
www.manaraa.com

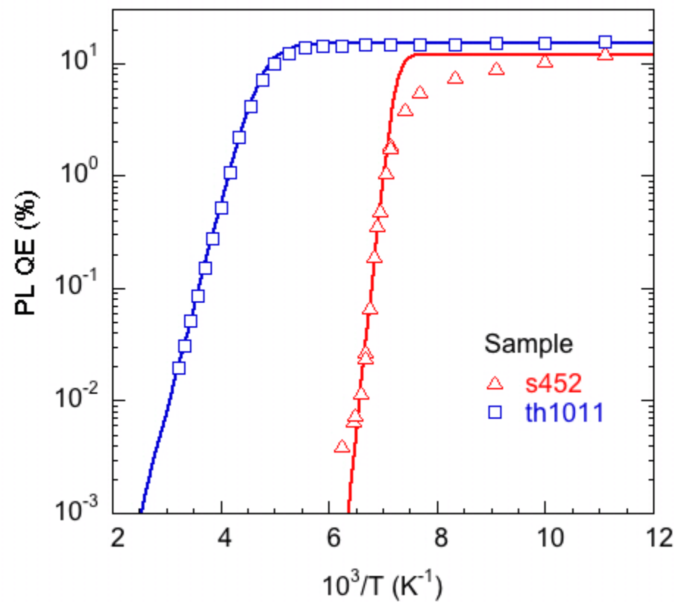

Fig. 3-3: Temperature dependence of the BL band quantum efficiency in undoped GaN (th1011, blue squares) and Zn-doped GaN (s452 , red triangles).

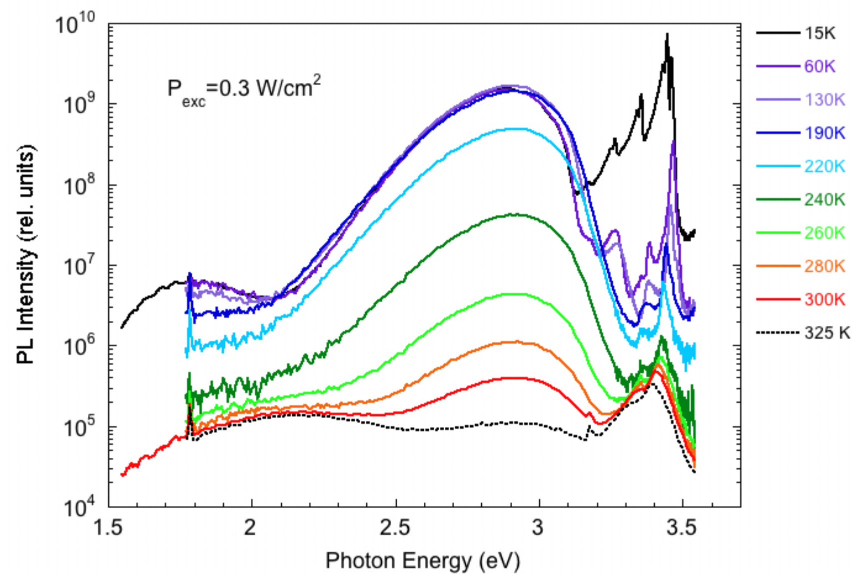

Fig. 3-4: PL spectra of Zn-doped GaN (ap274) in the temperature range of 15 to 325 K with P_{exc} = 0.3 W/cm^2.

المنارة للاستشارات
www.manaraa.com

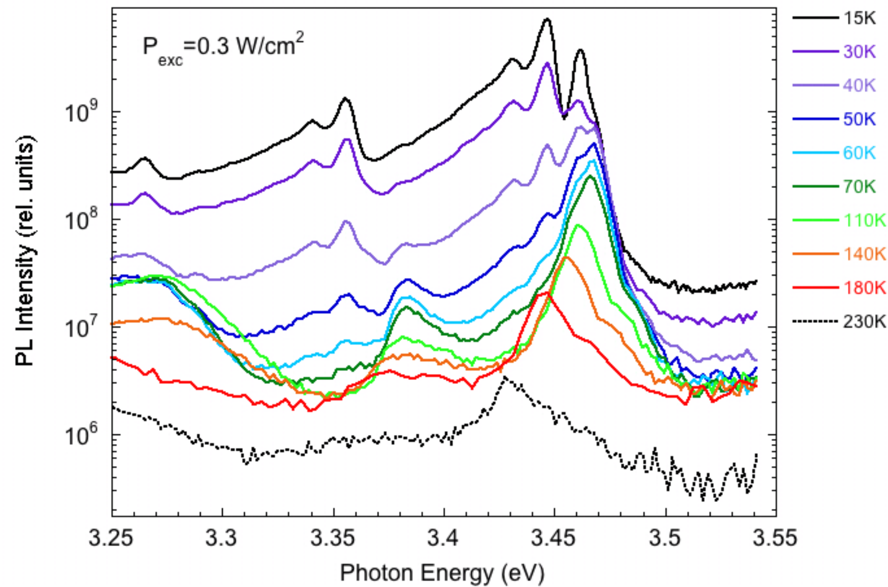

Fig. 3-5: PL spectra of the excitonic luminescence band and its LO phonon replica in the temperature range of 15 K to 230 K at $P_{exc} = 0.3$ W/cm^2.

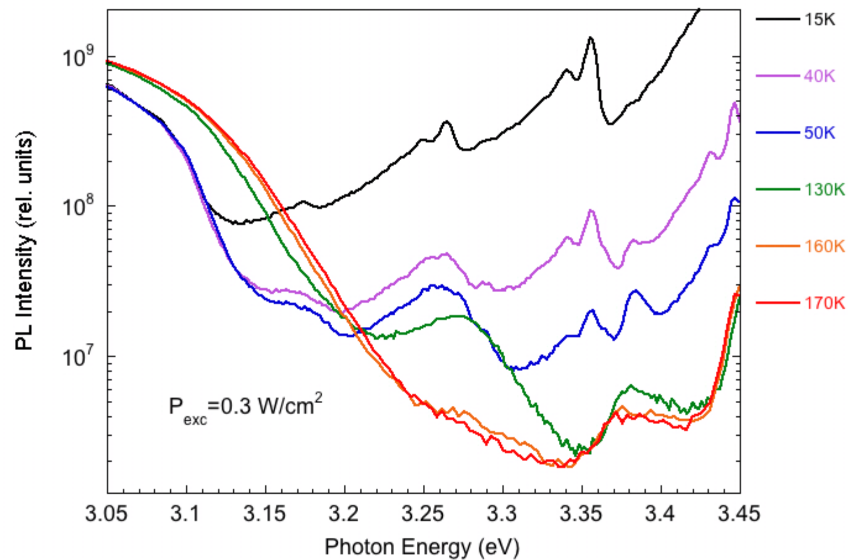

Fig. 3-6: PL spectra of the UVL band and its LO phonon replica in the temperature range of 15 K to 230 K at $P_{exc} = 0.3$ W/cm^2.

المنارة للاستشارات
www.manaraa.com

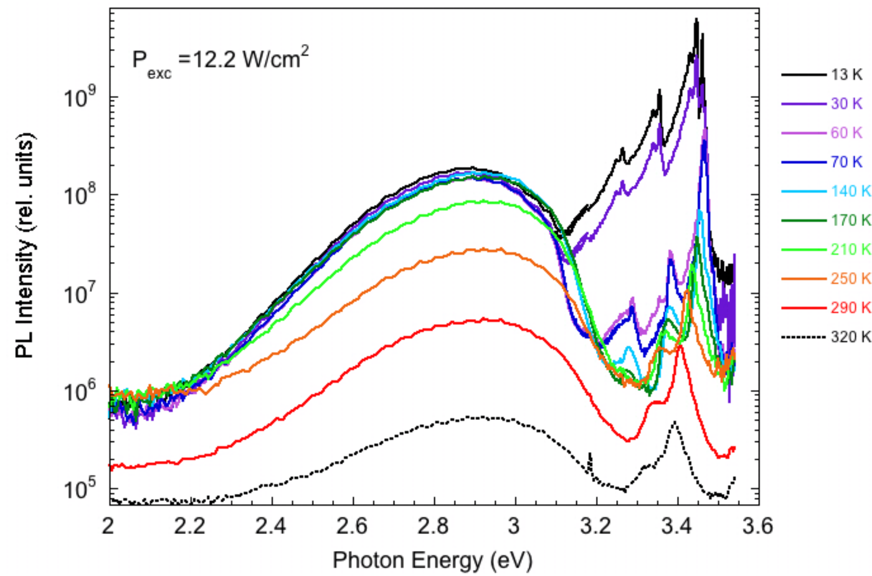

Fig. 3-7: PL spectra of Zn-doped GaN (ap274) in the temperature range of 15 to 320 K with P_{exc} = 12.2 W/cm^2.

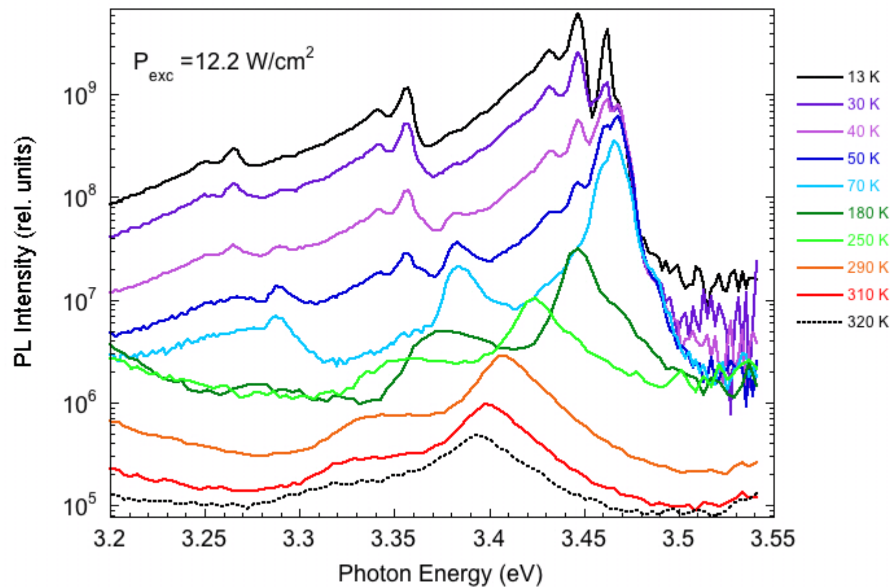

Fig. 3-8: PL spectra of the excitonic luminescence band, UVL band and their LO phonon replicas in the temperature range of 13 K to 230 K at P_{exc} = 12.2 W/cm^2.

المنارة للاستشارات
www.manaraa.com

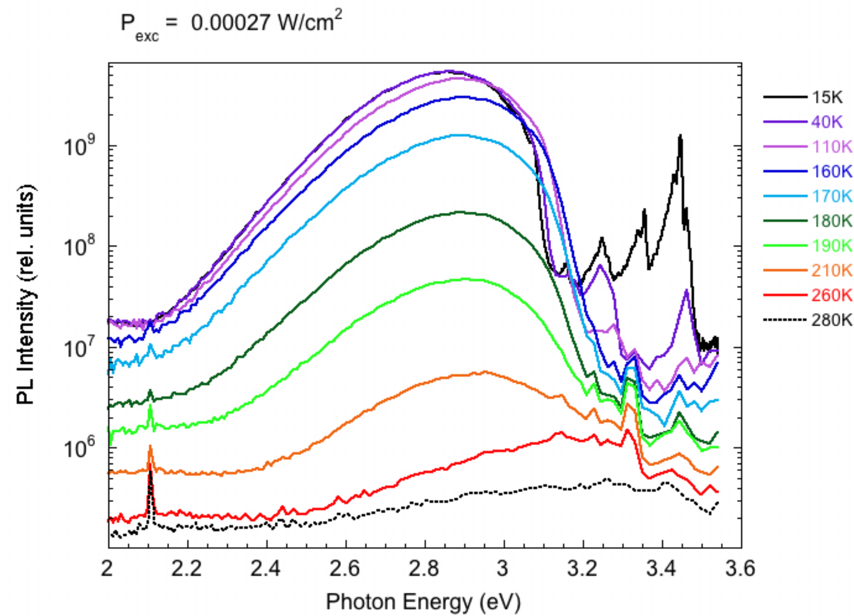

Fig. 3-9: PL spectra of Zn-doped GaN (ap274) in the temperature range of 15 to 280 K with P_{exc} = 0.00027 W/cm^2.

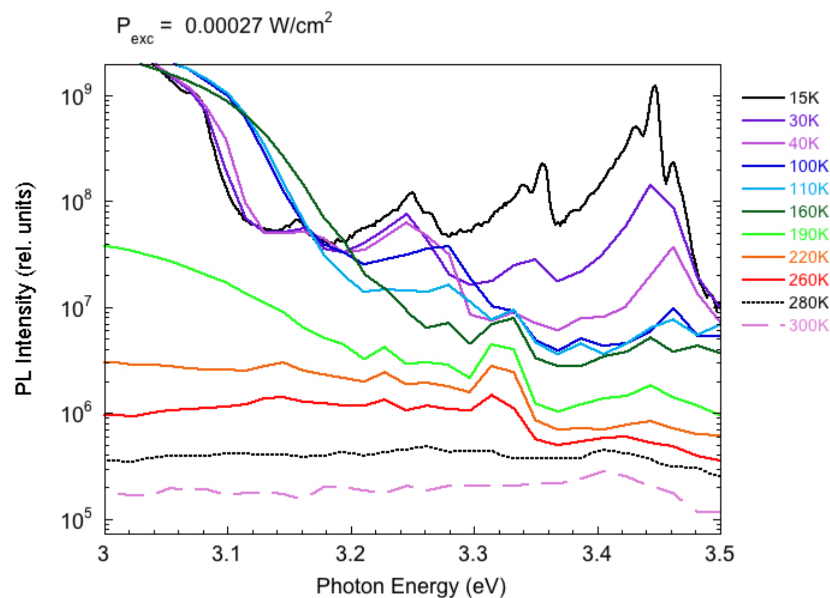

Fig. 3-10: PL spectra of the excitonic luminescence band, UVL band and their LO phonon replicas in the temperature range of 13 K to 300 K at P_{exc} = 0.00027 W/cm^2.

المنارة للاستشارات
www.manaraa.com

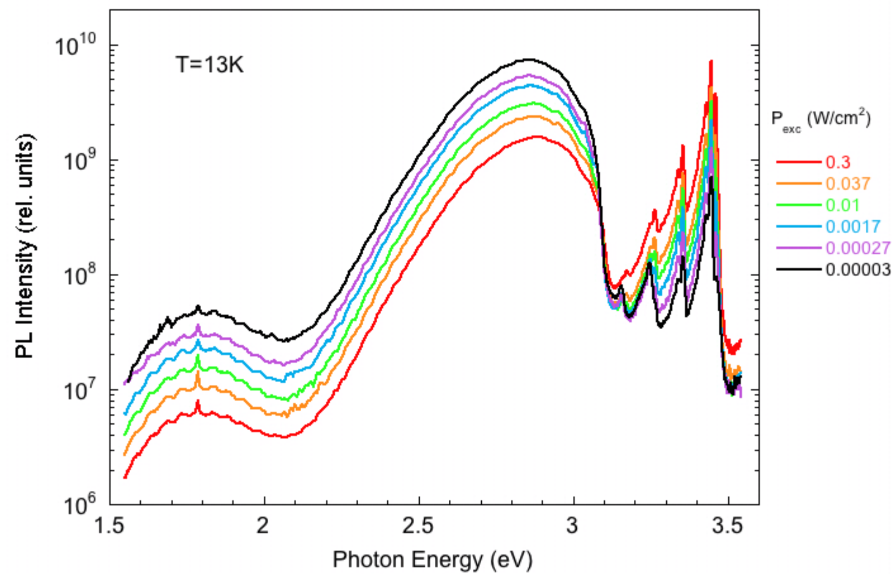

Fig. 3-11: Normalized PL spectra of Zn-doped GaN (ap274) at the temperature of 13 K with excitation intensity ranging from 0.3 to 0.00003 W/cm^2. PL intensity is divided by the excitation intensity.

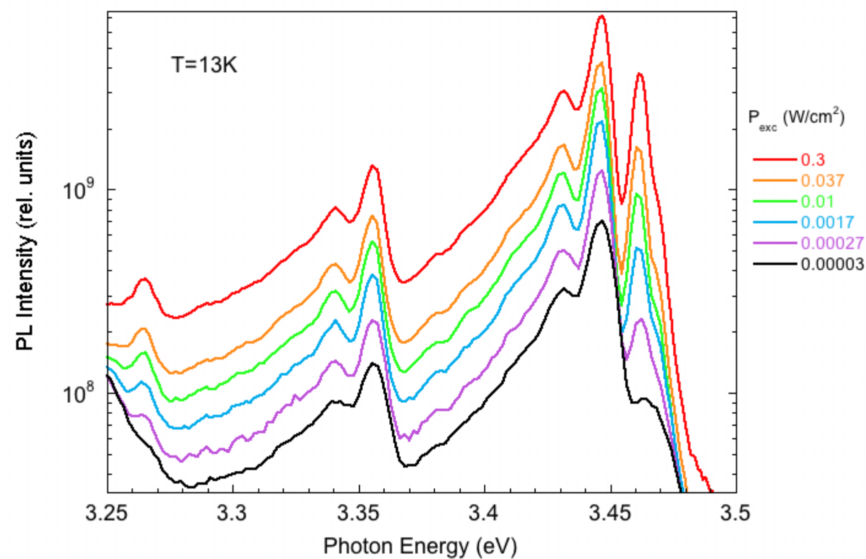

Fig. 3-12: Normalized PL spectra of the excitonic luminescence band and its LO phonon replica in the excitation intensity range of 0.3 to 0.00003 W/cm^2.

المنارة للاستشارات
www.manaraa.com

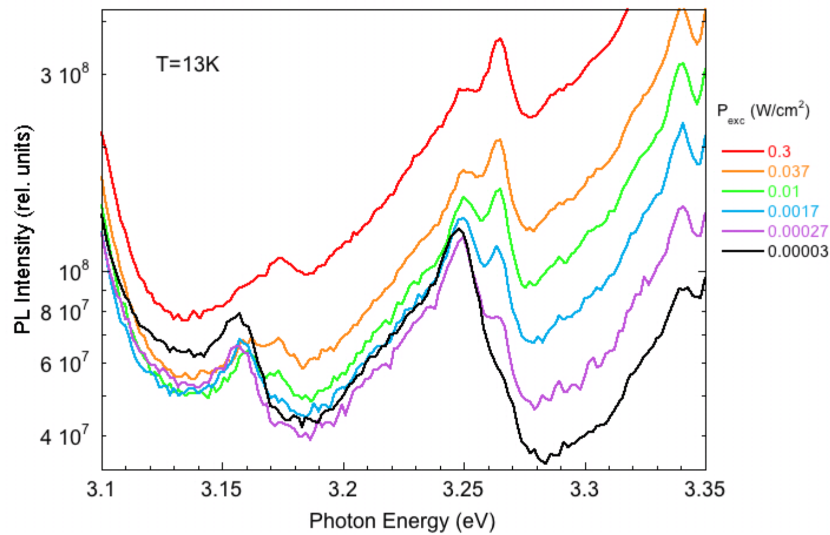

Fig. 3-13: Normalized PL spectra of the UVL band and its LO phonon replica in the excitation intensity range of 0.3 to 0.00003 W/cm^2.

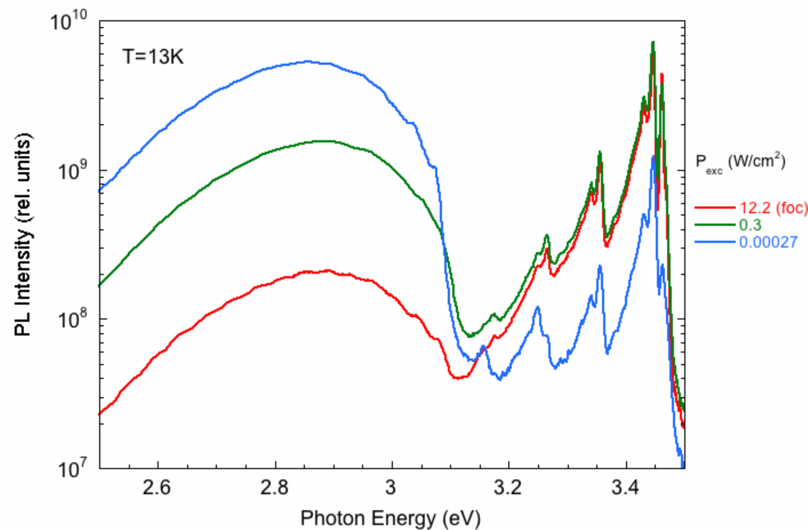

Fig. 3-14: Normalized PL spectra of Zn-doped GaN (sample ap274) at excitation intensities of 12.2, 0.3 and 0.00027 W/cm^2.

www.manaraa.com

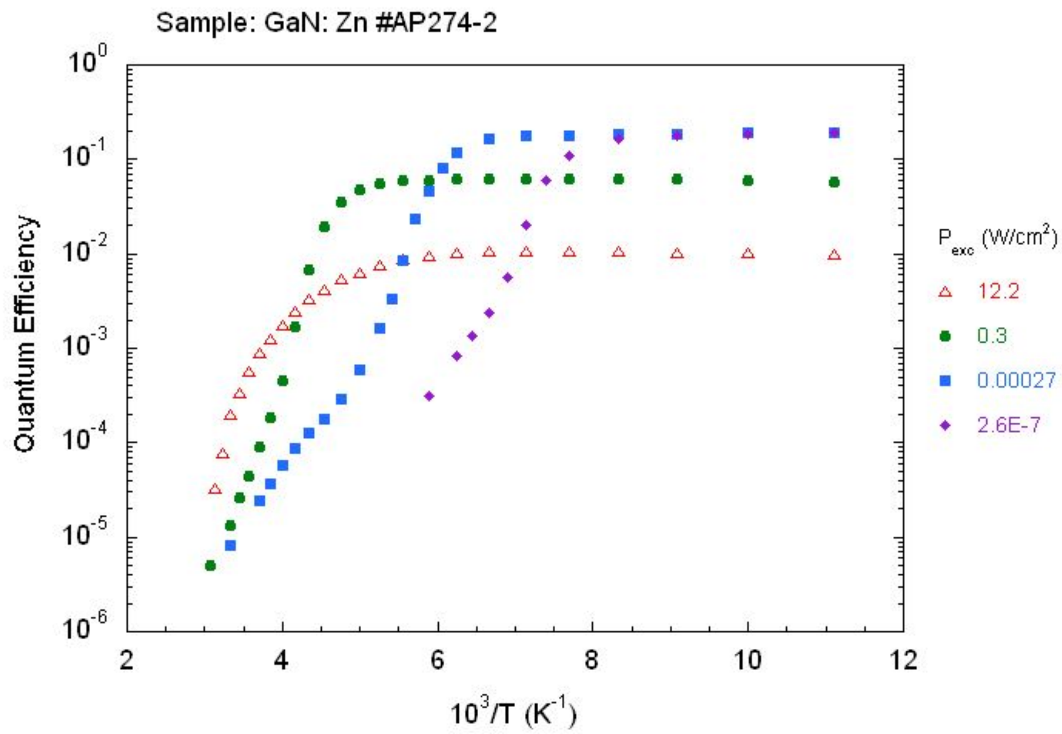

Fig. 3-15: Quantum efficiency of the BL band for P_{exc} from 12.2 4o 2.6×10^{-7} W/cm^2.

المنارة للاستشارات
www.manaraa.com

Chapter 4. Phenomenological Model

4.1 Rate Equations

The most basic model that can be suggested for a semiconductor, in particular, for undoped and Zn-doped GaN samples, consists of three types of point defects. These are an acceptor, a shallow donor and a nonradiative center (donor or acceptor). It is the minimum set considered because the PL usually involves shallow donors and different acceptors, whereas nonradiative centers must be included to account for lower than 100% quantum efficiency of PL. Point defects usually act as donors or acceptors, depending on whether they donate electrons to or accept them from the crystal lattice. Hereafter, acceptors and shallow donors will be labeled with the letters A and D, respectively. Acceptors A have a concentration of N_A and ionization energy of E_A. An acceptor can either be neutral (A^0) when it binds a hole or negatively charged acceptor (A^-) when it captures an electron. The energy level of an acceptor will be labeled as $A^{0/-}$, as seen in Fig. 4-1. Shallow donors D have a concentration of N_D and ionization energy of E_D. A donor with a level $D^{+/0}$ can either be a neutral donor D^0 (electron is bound), or positively charged donor D^+ that has lost one electron. The last species is an unknown nonradiative center S that may be either a donor or an acceptor with a concentration of N_S with a deep energy level position of which is unknown. Supposing that the nonradiative center $S^{+/0}$ is a donor, then S^0 is a neutral center and S^+ is a positively charged center that has lost an electron. Alternately, the S center could be an acceptor and $S^{+/0}$ would be replaced with $S^{0/-}$ where S^- is a negatively charged acceptor that has captured an electron.

www.manaraa.com

The concentrations of *A*, *D*, and *S* centers in different charge states are N_A^0 for neutral acceptors, N_A^- for negatively charged acceptors, N_D^0 for neutral donors, N_D^+ for positively charged donors, N_S^0 for neutral nonradiative centers, and N_S^+ for positively charged nonradiative centers. The sum of both charge states is the concentration for each level of N_A, N_D, and N_S.

Next we will introduce a generation rate *G*, which is the number of electron-hole pairs per unit volume produced per unit time by a continuous illumination on the samples. There are two methods used for obtaining *G*. In the first method, *G* is derived from the excitation power as

$$G = \frac{P_0}{L_{eff}}, \tag{11}$$

where P_0 is the laser intensity in units of $\frac{\text{photons}}{\text{cm}^2\text{s}}$ and L_{eff} is the width of an effective layer in the material where the laser light is mostly absorbed. In GaN, the laser light is mostly absorbed in the layer $L_{eff} = \alpha^{-1}$ which is approximately 100 nm or 10^{-5}cm.[10] The second method accounts for a gradual decrease of the excitation light in a sample and entails the absorption coefficient of $\alpha \approx 1.5 \times 10^5\, cm^{-1}$ in acquiring *G*. The intensity of laser light decreases exponentially from the surface and at a distance *x* is represented by $P_0 e^{-\alpha x}$. In a given layer of material (Δx) the amount of light intensity that is absorbed is

$$\Delta P(x) = \alpha P_0 e^{-\alpha x} \Delta x\,. \tag{12}$$

Therefore, the generation rate can be found by the integral of

$$G = \int_o^D \alpha P_0 e^{-\alpha x}\, dx\,, \tag{13}$$

where *D* is the thickness of the GaN layer grown on the substrate. Attenuating laser illumination with neutral-density filters may vary this excitation rate proportionally to the filter transparency.

المنارة للاستشارات

www.manaraa.com

The generated electron-hole pairs recombine through various channels. In steady state, the rate at which electrons escape from the conduction band depends on the rates of capture or recombination via various energy levels of defects and impurities. Transition rates of charge carriers (electrons and holes) transferring from one state to another are calculated by direct multiplication of the capture coefficient, concentration of available carriers and concentration of available empty sites, given as $C_{ab}N_1N_2$ The capture coefficient (C_{ab}) is a constant with subscripts indicating the transition from the initial state (subscript *a*) to the final state (subscript *b*), N_1 is the concentration of available carriers and N_2 is the concentration of available sites for these carriers. Electrons from the conduction band are captured by acceptor, shallow donor and nonradiative centers at rates of $C_{nA}N_A^0 n$, $C_{nD}N_D^+ n$, and $C_{nS}N_S^+ n$. Holes from the valance band are captured by acceptors and nonradiative centers at rates of $C_{pA}N_A^- p$ and $C_{pS}N_S^0 p$. There is a low probability for holes to be captured by neutral shallow donors, *D*, due to the fact that neutral donors do not attract holes. Acceptors are filled with electrons in dark and are very efficient in attracting holes, and some *S* centers have been experimentally observed to compete with the efficiency of acceptors. Therefore, the probability of a hole being captured by acceptors or *S* centers is extremely high in comparison to shallow donors. The rate of holes being captured by shallow donors is negligible and not taken into consideration in the rate equations. There are also transitions of electrons from shallow donor levels to acceptor levels at a rate of $C_{DA}N_D^0 N_A^0$.

Another factor of transition that arises in these rates of flow is a result of thermal excitation causing trapped electrons to be emitted to the conduction band at a rate of Q_D or trapped holes to be emitted to the valence band at a rate of Q_A. The rate of these processes is given by the following equations

المنارة للاستشارات

www.manaraa.com

$$Q_A = \frac{C_{pA} N_V}{g} \exp\left[-\frac{E_A}{k_B T}\right], \tag{14}$$

$$Q_D = \frac{C_{nD} N_C}{g} \exp\left[-\frac{E_D}{k_B T}\right]. \tag{15}$$

The product of a capture coefficient (C_{pA} or C_{nD}) and the density of states (N_V or N_C) are divided by a degeneracy factor g. The degeneracy factor accounts for the electron spin. The effective density of states N_C in the conduction band and N_V in the valence band are functions of temperature and defined in the equations below as:

$$N_C = 2\frac{(2\pi m_n k_B T)^{3/2}}{(2\pi\hbar)^3}\,, \tag{16}$$

$$N_V = 2\frac{(2\pi m_p k_B T)^{3/2}}{(2\pi\hbar)^3}\,, \tag{17}$$

where T is temperature, k_B is the Boltzmann's constant, $\hbar$ is the Planck constant, m_n is the effective mass of an electron and m_p is the effective mass of a hole. The effective masses for GaN are $m_n = 0.2m_0$ and $m_p = 0.8m_0$, where m_0 is the mass of an electron in vacuum. The negative exponential term in Eqs. (14) and (15) consists of the binding energy of the acceptors E_A and the binding energy of donors E_D divided by the product of the Boltzmann's constant k_B and the temperature T in Kelvins.

For the model described above, there are several rate equations that describe transition balances under steady-state conditions. These rate equations consist of the balance of electrons in the conduction band, the balance of holes in the valence band, the neutrality equation of negatively charged and positively charged states, and the balance of transitions at the acceptor, donor and nonradiative energy levels.

المنارة للاستشارات
www.manaraa.com

The rate equation for the change in the conduction band of the free electron concentration is derived from the combination of free electrons generated from incident light illumination of samples at a rate G per unit volume and by emission by thermal excitation at a rate $Q_D N_D^0$ along with loses of free electrons from transitions to the acceptor level A at a rate of $C_{nA} N_A^0 n$, to the shallow donor D at a rate of $C_{nD} N_D^+ n$ and to the deep donor S at a rate of $C_{nS} N_S^+ n$. This balance in steady-state is given by

$$\frac{\partial n}{\partial t} = G - C_{nS} N_S^+ n - C_{nD} N_D^+ n - C_{nA} N_A^0 n + Q_D N_D^0 = 0, \qquad (18)$$

where C_{nA}, C_{nD}, and C_{nS} are the electron capture coefficients for the acceptor, shallow donor and the nonradiative center.

The rate of change in the valence band of the free hole concentration is derived from the combination of holes generated at a rate G and thermal emission from the acceptor level A at a rate of $Q_A N_A^0$ along with loses of holes from capture by the acceptor A at a rate of $C_{pA} N_A^- p$ and by the deep donor S at a rate of $C_{pS} N_S^0 p$. This balance in steady-state is given by

$$\frac{\partial p}{\partial t} = G - C_{pS} N_S^0 p - C_{pA} N_A^- p + Q_A N_A^0 = 0, \qquad (19)$$

where C_{pA}, C_{pD}, and C_{pS} are the hole capture coefficients for the acceptor, shallow donor and the nonradiative center.

The neutrality equation, that accounts for all positive and negative charge states, balances the sum of concentrations of holes p, positive nonradiative centers N_S^+, and single-charged donors N_D^+ with the sum of concentrations of electrons n and negative acceptors N_A^- and is given below

المنارة للاستشارات
www.manaraa.com

$$p + N_S^+ + N_D^+ = n + N_A^- . \tag{20}$$

The balance of transitions at the acceptor level contains the sum of holes recombining with electrons from the donor level and the flow of electrons from the conduction band to the acceptor level in equality to flow of holes to the acceptor level minus the thermal emission of holes to the valence band as shown below:

$$C_{DA} N_D^0 N_A^0 + C_{nA} N_A^0 n = C_{pA} N_A^- - Q_A N_A^0 . \tag{21}$$

The balance of transitions at the donor level is the flow of electrons from the conduction band to the donor minus the thermal emission of electrons from the donor level to the conduction band is equal to the recombination of electrons from the donor level with holes in the acceptor level as given below

$$C_{nD} N_D^+ n - Q_D N_D^0 = C_{DA} N_D^0 N_A^0 . \tag{22}$$

For the nonradiative center, there is a balance of the transition rate of electrons from the conduction band to the transition rate of holes from the valence band, stated below

$$C_{nS} N_S^+ n = C_{pS} N_S^0 p . \tag{23}$$

This model becomes more advanced with an increase in observable levels that can be seen in data acquired from PL experiments. The range of spectra observed for particular materials will give cause to the addition of donor and acceptor levels. Mathematica programs, beginning with the most basic model, have been developed to incorporate these additional levels and assist in interpreting concentration and energy levels of defects within semiconductors by comparing experimental data with the rate equation theory.

المنارة للاستشارات
www.manaraa.com

4.2 Abrupt Tunable Quenching of PL

The Arrehenius plot of undoped GaN compared with Zn-doped GaN was previously shown. The activation energies obtained from this plot were 0.35 eV for the undoped and 1.0 eV for the Zn-doped GaN. This would indicate a contradiction in the defect responsible being the same for both cases. What is even more peculiar, though, is that a defect with this deep acceptor level could not produce a BL. A rate equation model was developed that describes the temperature dependence of photoluminescence in GaN. This model explains this strange behavir as abrupt tunable quenching of PL with Zn as the acceptor. In the model, the activation of the defect is the same for both the undoped and Zn-doped GaN. It is the thermal processes that increase the abruptness of the quenching along with excitation dependence of quenching temperatures.

The explanation of the abrupt thermal quenching is as follows: In dark, the conduction band and S centers are empty of free electrons. Under illumination at low temperatures, the S centers become saturated with electrons. This saturation prevents electron that have been excited to the conduction band from recombining with holes at the nonradiative center. Instead of nonradiative recombination, the electrons from the conduction band radiatively recombine with the acceptor levels. As temperature increases, the emission of thermally excited holes from the acceptor level to the valence band increases significantly. With this increase of holes in the valence band, these holes are available for recombination with electrons at the S centers and the S channel becomes unblocked. This dramatically decreases the amount of electrons in the conduction band by orders of magnitude and as a result the PL intensity also abruptly drops.

المنارة للاستشارات
www.manaraa.com

This model includes several nonlinear equations that would be extremely challenging to solve without the help of a useful program like that the ones we developed using Mathematica. A complete explanation of this program is given in Appendix A. Previously estimated concentrations of native defects, impurities, and complexes seen in literature can be verified or elucidated with the use of this model when comparing theoretical results with experimental data. This program will assist in discovering the origins of various PL bands and how doping effects the intensity of these peaks, which has remained a controversial issue despite extensive studies in this area.

المنارة للاستشارات
www.manaraa.com

Chapter 4 Figures

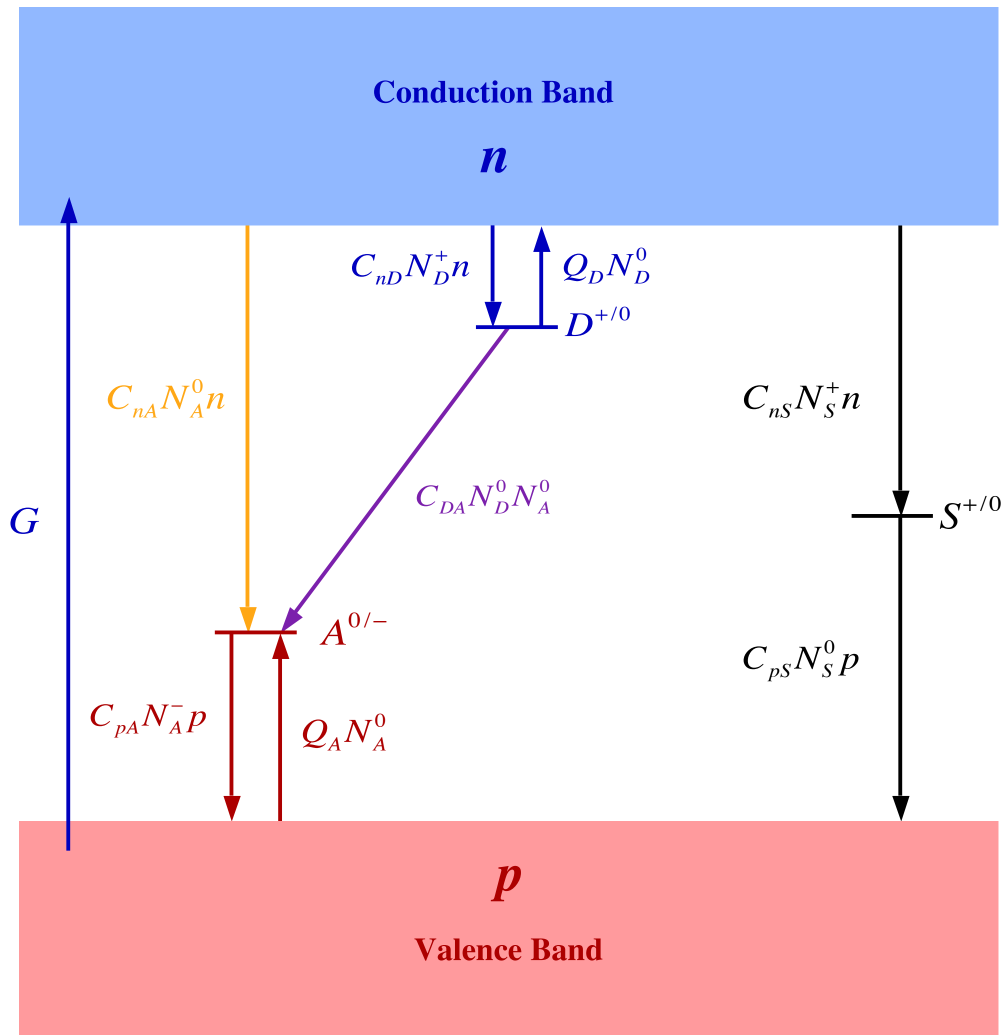

Fig. 4-1: Basic band diagram and main transitions of electrons for a semiconductor with a shallow donor (*D*), acceptor (*A*), and a nonradiative deep donor (*S*).

www.manaraa.com

Chapter 5. Comparison of Theory with Experiment

Using this model allows us to interpret the unusual behavior of PL observed in our sample. Temperature dependence and thermal quenching seen in experimental results can be analyzed with recombination statistics to interpret this effect and give additional information about the properties that contribute to these peaks. A comparison is made between a quantum efficiency vs. $10^3/T$ graph obtained from experiment and one calculated using Mathematica (see Fig. 5-1) by adjusting parameters to effectively mimic the same characteristics. The parameters entered into the program have well established estimated parameters fixed and adjustments are applied to parameters that have varying values in documented reports. Although the fitting is not an exact match, it does mimic the major characteristics of abrupt thermal quenching of PL based on excitation intensity. By evaluating the shifts with varying intensity, acceptor and donor concentrations in GaN can be determined, along with the rates at which they contribute to luminescence spectra.

Several point defects contribute to the radiative and non radiative mechanisms involved in GaN. This can become extremely complicated when dealing with multiple rate equations but can be reduced to a three-defect model to explain the behavior of one band of PL. The minimal set of centers involved in carrier recombination in Zn-doped GaN samples grown by HVPE consists of three types of point defects. These defects are the Zn_{Ga} acceptor, the O_N shallow donor, and an unknown nonradiative center. Zn_{Ga} is the dominant acceptor involved in the PL process in this sample and has an ionization energy of about 350 meV at temperatures between 100 and 300 K. The electron- and hole-capture coefficients C_{nA} and C_{pA} of the acceptor have been approximated by previous studies as 4×10^{-13} and 1×10^{-6} cm^3/s[10] and the upper limit of concentration was found by SIMS to be 1.7×10^{17} cm^{-3}. The dominant shallow donor in undoped

المنارة للاستشارات
www.manaraa.com

GaN is the O_N shallow donor as a result of contamination during the growth process. The contamination is expected to increase when the sample is doped with a Zn acceptor. The concentration for the O_N donor in undoped GaN is in the 10^{17} cm^{-3} range. The recombination emission that is observed in a transition from the O_N donor to the Zn_{Ga} acceptor is a DAP transition seen in the BL band. Since concentration is focused on one band of interest, other PL bands are regarded as nonradiative and are incorporated into the *S* center. This could explain the discrepancy in the fits between experimental and theoretical graphs. We assume that the nonradiative center is a simple deep donor and, although the capture parameters and concentration are unknown, they are given reasonable parameters. The values used in fitting the Mathematica to the experimental quantum efficiency (QE) graphs are $N_A = 9.35 \times 10^{16}$, $N_S = 8.5 \times 10^{16}$, $N_D = 8.5 \times 10^{15}$ (all in cm^{-3}); $C_{nS} = 10^{-7}$, $C_{nD} = 10^{-8}$, $C_{pS} = 5 \times 10^{-7}$, $C_{pA} = 10^{-6}$, $C_{nA} = 10^{-11}$, $C_{DA} = 10^{-11}$ (all in cm^3/s) and $E_D = 30$ meV, $E_A = 340$ meV, as seen in Fig. 5-1. The positions of the abrupt thermal quenching of QE in the experimental and theoretical graphs are very similar. With the decrease in intensity, the calculated dependences mimic the increase in QE and the decrease in thermal quenching temperature. This is a result of the various mechanisms that are occurring with other PL bands in the spectra but the values acquired from Mathematica programs with this type of fit give us a fairly precise approximation to the mechanisms involved in the band of focus.

Further programs have been created to analyze two or more bands. By mastering the basic model version of a Mathematica program to determine properties and dynamics of GaN, future use of more complicated programs to assist in PL analysis will be extremely beneficial. This is due to the accuracy that can be obtained from a computer program by simultaneous solving several nonlinear equations involved in the mechanism of PL in GaN.

المنارة للاستشارات
www.manaraa.com

Chapter 5. Figures

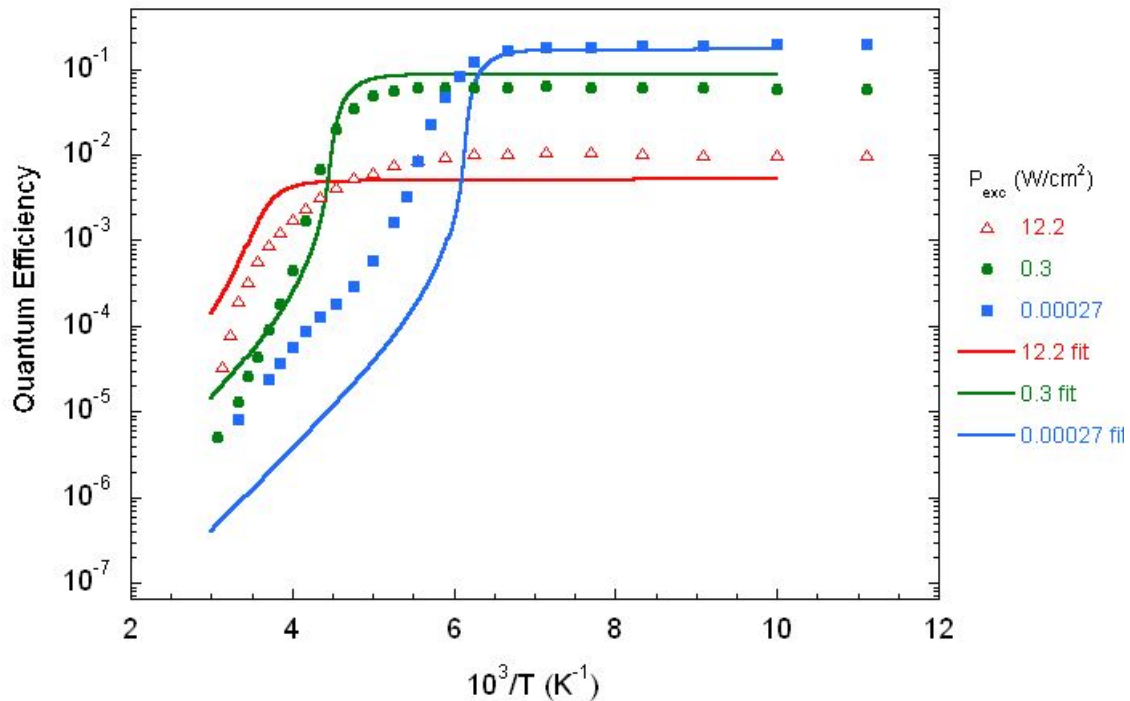

Fig. 5-1: Theoretical fit with experimental data for P_{exc} of 12.2, 0.3 and 0.00027 W/cm^2. Parameters for fit were $N_A = 9.35 \times 10^{16}$, $N_S = 8.5 \times 10^{16}$, $N_D = 8.5 \times 10^{15}$ (all in cm^{-3}); $C_{nS} = 10^{-7}$, $C_{nD} = 10^{-8}$, $C_{pS} = 5 \times 10^{-7}$, $C_{pA} = 10^{-6}$, $C_{nA} = 10^{-11}$, $C_{DA} = 10^{-11}$ (all in cm^3/s) and $E_D = 30$ meV, $E_A = 340$ meV.

www.manaraa.com

Chapter 6. Summary

There are many applications in several different market avenues that can utilize the unique characteristics of GaN. Because of the usefulness of GaN, investigating its properties and processes will enhance the understanding of this material. As a result, the effects of impurity doping will be utilized, and the growth techniques will improve. Extensive research has been done in this area but very little has been concretely determined about the complex dynamics of the processes involved. Photoluminescence (PL) is a useful tool in observing the optical functions of GaN when it is under illumination. The intentional introduction of impurity defects in GaN changes or enhances the spectra observed in PL, and these behavioral changes can be useful in developing an explanation for their effect on the material.

PL spectra taken of Zn-doped GaN and compared with undoped GaN spectra show distinct behavioral changes in one of the only PL bands whose origin has been previously determined. This is the blue luminescence (BL) band and has been attributed to a Zn_{Ga} acceptor. Zn-doped GaN shows a dramatic thermal quenching in comparison with undoped GaN. To understand this behavioral change, PL spectra were taken from Zn-doped GaN for further observation. Spectra of PL with temperature variation were experimentally obtained, and then the excitation intensity was varied for additional temperature dependence observation. What was observed, with the variation of excitation intensity, was the shift in the temperature where abrupt thermal quenching of the BL band occurred. The maximum of PL intensity was also shown to be dependent on excitation intensity. Lower maximum PL intensities combined with higher temperatures of thermal quenching occurrence were seen at higher excitation intensities. Higher maximum PL intensities with thermal quenching happening at lower temperatures were seen at

www.manaraa.com

lower excitation intensities. This step-like process was another strange behavioral characteristic of the Zn-doped GaN.

To explain the unusual behavior observed in the PL of Zn-doped GaN, a basic rate equations model was proposed for a theoretical view and interpretation of the dynamics involved. This model was incorporated into a mathematical modeling program created with Mathematica software. The results of theoretical calculations were compared to and fitted with experimental data. Although a complete match was not obtained, the experimental and theoretical graphs of the quantum efficiency of PL of the BL band efficiently mimic each other with step-like shifts of intensity and temperature values of thermal quenching occurrence with the change in excitation intensity.

The basic model, that was theoretically proposed, is a simplified version of the processes involved in the PL of Zn-doped GaN. This model consists of only three defect levels and the addition of defect levels and their contributions can be applied for further investigation. The simplicity of this model may also account for the discrepancies seen in the fitting of the theoretical results with the experimental results. The values obtained from the simplified model are not only reasonable parameters according to previous studies but can be utilized in more advanced programs that have been created to account for additional properties. This theoretical model and the mathematical modeling programs that were created as an analytical tool for the comparison of this explanation with experimental data can be utilized in investigating the properties and processes involved with point defects within the GaN crystal structure.

المنارة للاستشارات
www.manaraa.com

References

1. I. Akasaki and H. Amano "Crystal Growth and Conductivity Control of Group III Nitride Semiconductors and Their Application to Short Wavelength Light Emitters". *Jpn. J. Appl. Phys.* **36**, 5393–5408 (1997).
2. A. Lidow, J. B. Witcher, and K. Smalley. "Enhancement Mode Gallium Nitride (eGaN) FET Characteristics under Long Term Stress". GOMAC Tech Conference (March 2011).
3. "Gallium Nitride-Based Modules Set New 180-Day Standard For High Power Operation." *Northrop Grumman*, 13 April 2011.
4. S. A. Jewett, M. S. Makowski, B. Andrews, M. J. Manfra, and A. Ivanisevic. "Gallium nitride is biocompatible and non-toxic before and after functionalization with peptides". *Acta Biomaterialia* **8**, 728-733 (2012).
5. Pierre Gilbart. *Rep. Prog. Phys.* **67**: 667-715 (2004).
6. V. Dmitriev and A. Usikov, III-Nitride Semiconductor Materials, *Technologies and Devices International, Inc.* MD
7. A. Y. Cho and J. R. Arthur Jr., "Molecular beam epitaxy". *Prog. Solid State Chem.* **10**, 157–192 (1975).
8. W. C. Hughes, W. H. Rowland, Jr., M. A. L. Johnson, S. Fujita, J. W. Cook and J. F. Schetzina. *J. Vac. Sci. Technol. B* **13**, 4 (1995).
9. S. A. Cambell, *The Science and Engineering of Microelectronic Fabrication*, Oxford University Press, New York City, pg. 391-429 (2001).
10. M. A. Reshchikov and H. Morkoc. *J. Appl. Phys.* **97**, 061301 (2005).

المنارة للاستشارات
www.manaraa.com

11. S. Limpijumnong and C. G. Van de Walle. *Phys. Rev. B* **69**, 035207 (2004).

12. C.G. Van de Walle and J. Neugebauer. *J. Appl. Phys.* **95**, 3851 (2004).

13. J. I. Pankove and J. A. Hutchby, *J. Appl. Phys.* **47**, 5387 (1976).

14. J. Oila *et al.*, *Appl. Phys. Lett.* **82**, 3433 (2003).

15. T. Ogino and M. Aoki, *Jpn. J. Appl. Phys.* **19**, 2395 (1980)

16. E. F. Schubert, I. D. Goepfert, and J. M. Redwing, *Appl. Phys. Lett.* **71**, 3224 (1997).

17. R. Zhang and T. F. Kuech, *Appl. Phys. Lett.* **72**, 1611 (1998).

18. R. Dingle and M. Ilegems, *Solid State Commun.* **9**, 175 (1971)

19. M. A. Reshchikov and R. Y. Korotkov, *Phys. Rev. B* **64**, 115205 (2001).

20. H. C. Yang, T. Y. Lin, and Y. F. Chen, *Phys. Rev.* B **62**, 12593 (2000).

21. B. Han, J. M. Gregie, and B. W. Wessels, *Phys. Rev. B* **68**, 045205 (2003).

22. U. Kaufmann, M. Kunzer, M. Maier, H. Obloh, A. Ramakrishnan, B. Santic, and P. Schlotter, *Appl. Phys. Lett.* **72**, 1326 (1998).

23. C. Diaz-Guerra, J. Piqueras, and A. Cavallini, *Appl. Phys. Lett.* **82**, 2050 (2003).

24. A. P. Young and L. J. Brillson, *Appl. Phys. Lett.* **77**, 699 (2000).

25. L. S. Dang, K. M. Lee, G. D. Watkins, and W. J. Choyke, *Phys. Rev. Lett.* **45**, 390 (1980).

26. M. A. Reshchikov, G.-C. Yi, and B. W. Wessels, *Phys. Rev. B* **59**, 13176 (1999).

27. M. Leroux, N. Grandjean, B. Beaumont, G. Nataf, F. Semond, J. Massies, and P. Gibart, *J. Appl. Phys.* **8**, 3721 (1999).

28. M. A. Reshchikov, A. A. Kvasov, M. F. Bishop, T. McMullen, A. Usikov, V. Soukhoveev, and V. A. Dmitriev, *Phys. Rev. B* **84**, 075212 (2011).

المنارة للاستشارات
www.manaraa.com

A.1 Appendix

Mathematica program

Problem 4

By Anita J. Olsen

(Debug) In[6]:=
```
Needs["PhysicalConstants`"]
Needs["Units`"]
Needs["PlotLegends`"]
fBox = Function[DisplayForm[ FormBox[#, TraditionalForm]]];
tBox = Function[DisplayForm[ ToBoxes[#, TraditionalForm]]];
```

Analysis of Data

- **Parameter Values for Semi-Insulating GaN doped with Zn -- p-type**
- **Defect Species**

The material contains several defect species listed below with the various charge states indicated by the superscripts.

$A^{0/-}$ – an acceptor, for instance Zn instead of Ga
A^0 – neutral acceptor, vacancy is free
A^- – negative acceptor captured an electron
$S^{+/0}$ – nonradiative center (*a* donor)
S^0 – neutral center
S^+ – positive center lost an electron
$D^{+/0}$ – *a* donor
D^0 – neutral donor
D^+ – single – charged donor lost 1 electron

n – concentration of free electrons in conduction band
p – concentration of holes in valence band

$\beta = \frac{1}{k_B T}$, where k_B is the Boltzmann constant and T is the temperature in Kelvins

- **Concentrations of Defects**

N_A – concentration of radiative acceptors A
$N_A = N_A^0 + N_A^-$
N_D – concentration of shallow donors D
$N_D = N_D^0 + N_D^+$
N_S – concentration of nonradiative centers (donors) S
$N_S = N_S^0 + N_S^+$

www.manaraa.com

- **Capture Coefficients**

A capture coefficient C is defined in these rate equations as $\frac{dN_1}{dt} = C\, N_1\, N_2$.

C_{nS}
C_{nD}
C_{pS}
C_{pA}
C_{nA}
C_{DA}

- **Energy Levels**

E_D – donor energy
E_A – acceptor energy

- **Effective Densities of states in the conduction band and valence band**

N_C – conduction band density of states
N_V – valence band density of states
g – degeneracy factor

- **Critical Temperature and Light Intensity**

G – exitation intensity
T – temperature in Kelvins

- **Temperature factors**

$$Q_A = \frac{C_{pA} N_V}{g} \exp\left[-\frac{E_A}{k_B T}\right]$$

$$Q_D = \frac{C_{nD} N_C}{g} \exp\left[-\frac{E_D}{k_B T}\right]$$

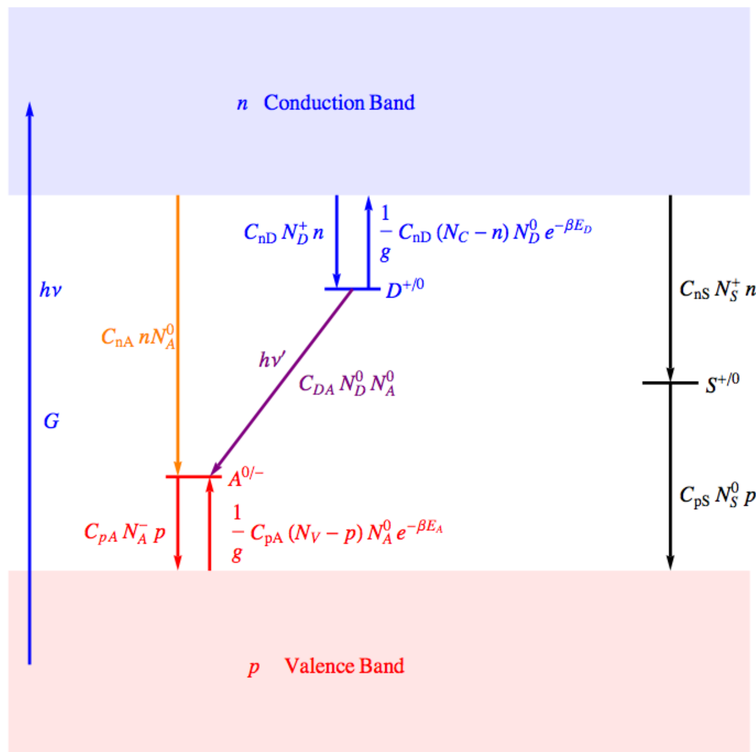

www.manaraa.com

▪ Defining Parameters in *Mathematica*

We get the Boltzmann constant from the Physical Constants package that is loaded at beginning of the paper.

```
(Debug) In[6]:= BoltzmannConstant
```

$$\text{(Debug) Out[6]=} \quad \frac{1.38065\times10^{-23}\ \text{Joule}}{\text{Kelvin}}$$

We are defining this Boltzmann constant in boltzmannIneVperK below because we need it to have a large number of significant figures (approximately 20) which is necessary for *Mathematica* to solve these equations.

```
(Debug) In[7]:= boltzmannIneVperK = 8.617343 × 10^-5 ElectronVolt / Kelvin
```

$$\text{(Debug) Out[7]=} \quad \frac{0.0000861734\ \text{ElectronVolt}}{\text{Kelvin}}$$

Here are the values of the defect concentrations in units of cm^{-3}.

```
(Debug) In[8]:= NS = 1.5 × 10^17;
                ND = 1.3 × 10^17;
                NA = 3.0 × 10^17;
```

Here are the values of the capture coefficients in units of $\frac{\text{cm}^3}{s}$.

```
(Debug) In[11]:= CnS = 1.0 × 10^-7;
                 CnD = 1.0 × 10^-8;
                 CpS = 3.0 × 10^-6;
                 CpA = 1.0 × 10^-6;
                 CnA = 4.0 × 10^-13;
                 CDA = 8.0 × 10^-12;
```

Here are the effective densities of states in the conduction and valence band in units of cm^{-3} and Kelvins , which are functions of temperature, and the degeneracy factor.

$$\text{(Debug) In[17]:=}\quad NC[\mathcal{T}_] := 1.57\times10^{19}\left(\frac{\mathcal{T}}{10^3}\right)^{3/2}$$

$$NV[\mathcal{T}_] := 1.0\times10^{20}\left(\frac{\mathcal{T}}{10^3}\right)^{3/2}$$

```
g = 2.0;
```

Here are the energy levels of acceptors and donors in units of meV.

```
(Debug) In[20]:= ℰD = 30.0;
                 ℰA = 340.0;
```

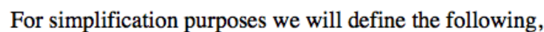

$$\mathcal{E}\text{DkB} = \frac{E_D}{k_B(1000\,K)}$$

$$\mathcal{E}\text{AkB} = \frac{E_A}{k_B(1000\,K)}$$

so that when these are multiplied by $\mathcal{T}\text{inv} = \frac{1000\ \text{Kelvin}}{\mathcal{T}}$ they give energy divided by $k_B\,\mathcal{T}$.

$$\text{(Debug) In[22]:=}\quad \mathcal{E}\text{DkB} = \text{Convert}\left[\frac{\mathcal{E}\text{D Milli ElectronVolt}}{\text{boltzmannIneVperK (1000 Kelvin)}}, 1\right]$$

```
(Debug) Out[22]= 0.348135
```

$$\text{(Debug) In[23]:=}\quad \mathcal{E}\text{AkB} = \text{Convert}\left[\frac{\mathcal{E}\text{A Milli ElectronVolt}}{\text{boltzmannIneVperK (1000 Kelvin)}}, 1\right]$$

```
(Debug) Out[23]= 3.94553
```

المنارة للاستشارات

www.manaraa.com

Here we have the temperature factors.

(Debug) In[24]:=

```
QD[𝒯_, 𝒩C_, δDkB_, CnD_, g_] := CnD 𝒩C/g Exp[-δDkB 1000/𝒯]
```

(Debug) In[25]:=

```
QA[𝒯_, 𝒩V_, δAkB_, CpA_, g_] := CpA 𝒩V/g Exp[-δAkB 1000/𝒯]
```

Here are semi-log plots of Q_D and Q_A versus $10^3\ K/T$ to see how they look.

(Debug) Out[26]=

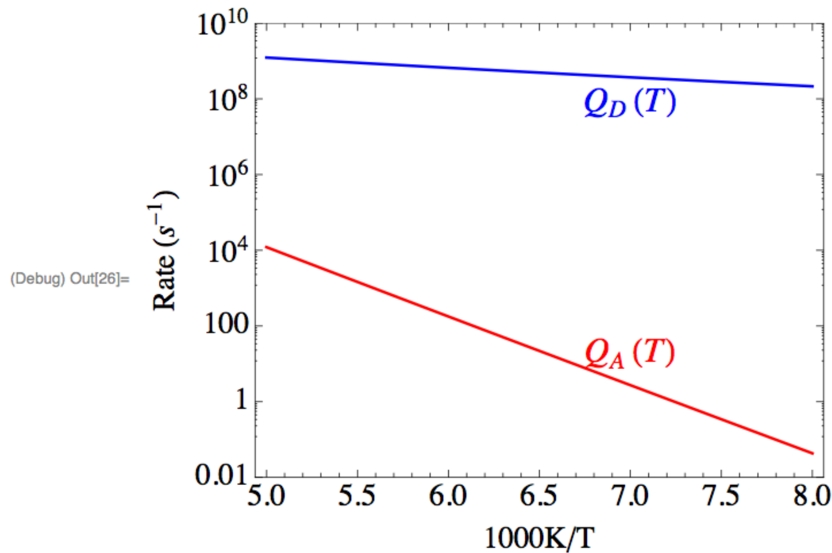

Thermal Effects

What has been observed in experimental data of, in this specific case, Zn doped GaN is that the photoluminescent intensity decreases significantly with increase in temperature. It is speculated that the thermal excitation of electrons from the valence band to the acceptor level produced by Zn doping leaves behind holes in the valence band. This is called quenching. The electrons from deep donors recombine with these holes nonradiatively and are therefore lost from the photoluminscent spectrum. Below is a model of this process for calculation purposes in *Mathematica*.

- **Rate equation model**
- **Defect Species**

First, I will introduce you to the defect species that are observed for a rate equation model used for interpretation of thermal effects.

This particular model of Zn impurities in GaN involves a total of four impurity and defect levels that are located within the bandgap. These are

A Zn acceptor. Zn is $4\,s^2$, Ga is $4\,s^2\,4\,p^1$, N is $2\,s^2\,2\,p^3$, so Zn_{Ga} lacks one electron in the charge-zero state. Energy ε_A is ~ 350 meV above valence band edge ε_V.

S Nonradiative center (a deep donor). Nature unspecified.

D Donor. The donor energy ε_D is ~ 30 meV below conduction band edge ε_C. Nature unspecified, but possibly a nitrogen vacancy. The level moves downward toward midgap as the charge state increases, $D^{+/0} \to D^{+/2+} \to D^{2+/3+}$.

If we remove the small density of electrons compared with the density of states of the conduction band and the small density of holes compared with the valence band, we have the picture below.

المنارة للاستشارات
www.manaraa.com

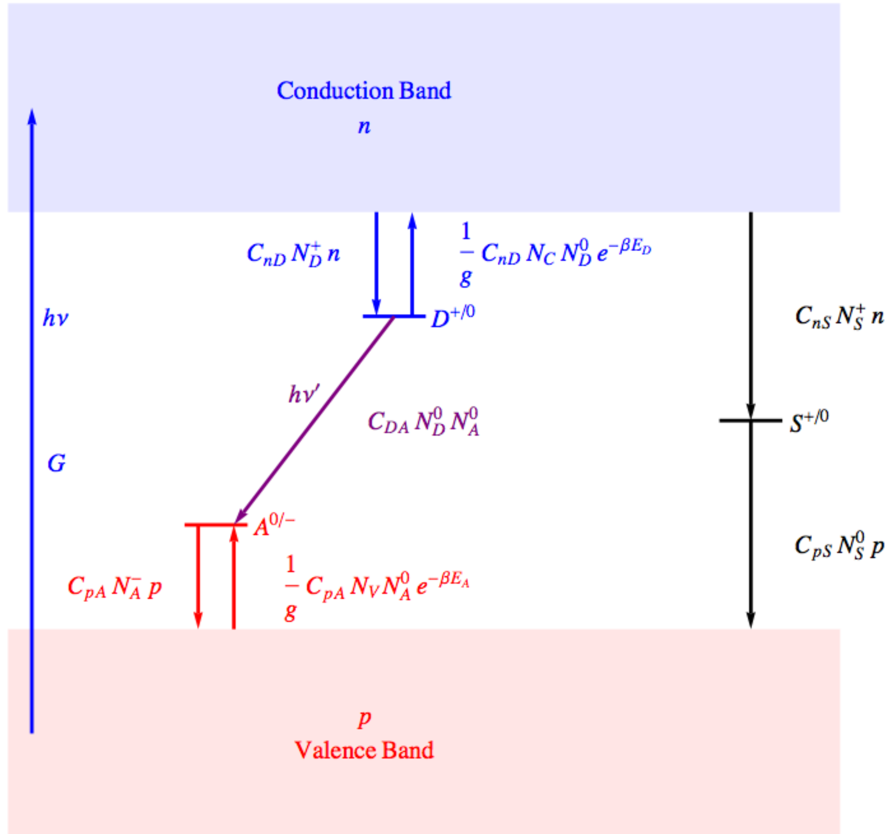

Next are the current rate equations for the flow of electrons through our band diagram above.

- **Rate Equations for the Model**

The rate equations generally involve two species, and are taken to be first order in each. There is also a condition of overall charge neutrality to be imposed. However, we use n to denote the density of electrons in the conduction band and p to denote the density of holes in the valence band. The "reactions" and their associated rate equations are summarized here.

The photogeneration rate G of electron-hole pairs is considered here to be constant,

$$h\nu \to n + p \;,\; \left(\frac{\partial n}{\partial t}\right)_{h\nu} = \left(\frac{\partial p}{\partial t}\right)_{h\nu} = G.$$

The rate equations are given by

Balance of electrons in the C.B.:	$\frac{\partial n}{\partial t} = G - C_{nS} N_S^+ n - C_{nD} N_D^+ n - C_{nA} N_A^0 n + Q_D N_D^0 = 0$	(1)
Balance of holes in the V.B.:	$\frac{\partial p}{\partial t} = G - C_{pS} N_S^0 p - C_{pA} N_A^- p + Q_A N_A^0 = 0$	(2)
Neutrality Equation:	$p + N_S^+ + N_D^+ = n + N_A^-$	(3)
Balance at D:	$C_{nD} N_D^+ n - Q_D N_D^0 = C_{DA} N_D^0 N_A^0$	(4)
Balance at S:	$C_{nS} N_S^+ n = C_{pS} N_S^0 p$	(5)
Balance at A:	$C_{DA} N_D^0 N_A^0 + C_{nA} N_A^0 n = C_{pA} N_A^- p - Q_A N_A^0$	(6)

المنارة للاستشارات
www.manaraa.com

In this discussion, we will neglect the transition of electrons from the conduction band to the acceptor level, which is given by the term $C_{na}\, n\, N_A^0$. Also, for all phases $N_D^+ \approx N_D$, although N_D^0 is still nonzero but very small. Here, $Q_D = \frac{C_{nD} N_C}{g} \exp\left[-\frac{E_D}{k_B T}\right]$ and $Q_A = \frac{C_{pA} N_V}{g} \exp\left[-\frac{E_A}{k_B T}\right]$.

Defining Rate Equations in *Mathematica*

If we rewrite the equations so that 0 is on the right hand we have the following definitions of the rate equations

```
(Debug) In[27]:= origEq1[GL_, n_, NA0_, ND0_, NSP_, ND_, QD_, CnA_, CnD_, CnS_] :=
  Module[{NDP},
   NDP = ND - ND0(* we are defining NDP here, followed by the definition of eq1*);
   GL - CnS NSP n - CnD NDP n  - CnA NA0 n  + QD ND0]

(Debug) In[28]:= origEq2[GL_, p_, NA0_, NSP_, NA_, NS_, QA_, CpA_, CpS_] :=
  Module[{NAM, NS0},
   NAM = NA - NA0;
   NS0 = NS - NSP;
   GL - CpS NS0 p - CpA NAM p  + QA NA0]

(Debug) In[29]:= origEq3[n_, p_, NA0_, ND0_, NSP_, NA_, ND_] :=
  Module[{NAM, NDP},
   NAM = NA - NA0;
   NDP = ND - ND0;
   p + NSP + NDP - n - NAM]

(Debug) In[30]:= origEq4[n_, NA0_, ND0_, ND_, QD_, CnD_, CDA_] :=
  Module[{NDP},
   NDP = ND - ND0;
   CnD NDP n - QD ND0 - CDA ND0 NA0]

(Debug) In[31]:= origEq5[n_, p_, NSP_, NS_, CnS_, CpS_] :=
  Module[{NS0},
   NS0 = NS - NSP;
   CnS NSP n -  CpS NS0 p]

(Debug) In[32]:= origEq6[n_, p_, NA0_, ND0_, NA_, QA_, CnA_, CpA_, CDA_] :=
  Module[{NAM},
   NAM = NA - NA0;
   CDA ND0 NA0 + CnA NA0 n - CpA NAM p  + QA NA0]
```

Calculation of carrier densities over a temperature range

```
(Debug) In[33]:=
TInvMin = 3.0;(*initial inverse temperature*)
TInvMax = 10.0;(*final inverse temperature*)
TInvinc = 0.02;(*increments for inverse temperature*)
Clear[n, p, NA0, ND0, NSP];
(* we are clearing previously entered values for the variables*)
TInvList = Range[TInvMin, TInvMax, TInvinc];(* this is 1000 Kelvin/T,
Range[first value, last value, increment]*)
TList = Map[1000/# &, TInvList];
(* Map makes a list of temperatures that converts the TInvList into
 temperature in Kelvin by replacing # by each individual temperature
 in TInvList. The resulting list has the same length as TInvList *)
Pexc = 2.0 × 10^-7 ;
GL = 1.6 × 10^23 Pexc;(* This is the generation rate G. We haven't put
 the units it but it would normally be concentration over unit time. *)
(*GL=3.2  10^16;
Pexc=GL/1.6  10^23*)
```

المنارة للاستشارات
www.manaraa.com

```
origEquationssolutionsCrossList =
  Map[Clear[n, p, NA0, ND0, NSP]; {n, p, NA0, ND0, NSP} /. NSolve[{FullSimplify[
        origEq1[GL , n ,
          NA0 , ND0 , NSP , ND, QD[#, NC[#], EDkB, CnD, g], CnA, CnD, CnS]] == 0,
      FullSimplify[origEq2[GL , p , NA0 , NSP , NA, NS,
          QA[#, NV[#], EAkB, CpA, g], CpA, CpS]] == 0,
      FullSimplify[origEq3[n , p , NA0 ,
          ND0 , NSP , NA, ND]] == 0,
      FullSimplify[origEq4[n , NA0 ,
          ND0 , ND,
          QD[#, NC[#], EDkB, CnD, g], CnD, CDA]] == 0,
      FullSimplify[origEq5[n , p ,
          NSP , NS, CnS, CpS]] == 0(*,
      FullSimplify[origEq6[n ,p ,
          NA0 ,ND0 ,NA,
          QA[#,NV[#],EAkB,CpA,g],CnA,CpA,CDA]]==0, This last equation is a linear
       combination of other equations and we keep it here in case we need it. *)},
     {n, p, NA0, ND0, NSP}, WorkingPrecision → 50] &, TList];
 (* This is where we solve the set of differential equations. NDSolve cannot deal
 with the units so we've canceled the units explicitly and the concentrations
 will come out without units, however, they are in units of cm^-3. *)
```

The following statement indexes (numbers) the solutions so that we will later be able to remove any temperatures for which a solution was not produced. We need to do this because the error messages indicates that there are temperatures for which NSolve could not solve the equations. We see messages about Overflow. Perhaps the use of normalized variables would prevent this, but then we wouldn't have our convenient symbols. Perhaps we could normalize before solving and put the factors back in after.

```
(Debug) In[42]:= indexedorigEquationssolutionsCrossList =
   MapIndexed[{#2[[1]], #1} &, origEquationssolutionsCrossList];
  (* This numbers the solutions so we can find where a solution
  was not produced. #1 is the set of solutions for one element in
  TInvList and #2 is the index for that element. This is given in {}
  format and #2[[1]] takes off the {}'s, giving us only index numbers*)
```

Here we pick the solution for which all the concentrations have physically reasonable values.

```
(Debug) In[43]:= SelectedOrigSolutionsCrossList =
   MapThread[{{#2[[1]], #1}, Flatten[Select[#2[[2]], #[[1]] ∈ Reals ∧ #[[1]] > 0 ∧ #[[2]] > 0 ∧ #[[3]] > 0 ∧
          #[[4]] > 0 ∧ #[[5]] > 0 ∧
          #[[3]] ≤ NA ∧ #[[4]] ≤ ND ∧
          #[[5]] ≤ NS &], 1]} &,
     {TInvList, indexedorigEquationssolutionsCrossList}];
  (* MapThread uses two lists. #1, in this case,
 corresponds to TInvList and #2 corresponds to indexedorigEquationssolutionsCrossList
   so we can take information from both lists. #2[[1]] means take the first element in
   the second list. Flatten[list,1] removes the outer pair of {} from the list. ∧
  means logical "and". Select[] gives us only the solutions
   that have physically reasonable parameters *)
```

Next we check to see if there are any temperatures for which a solution has not been found.

```
(Debug) In[44]:= CheckErrorPoints = Select[SelectedOrigSolutionsCrossList, #[[1]] == {} &]

(Debug) Out[44]= {}

(Debug) In[45]:= ErrorPoints = Map[{#} &, CheckErrorPoints[[All,1,1]]]

(Debug) Out[45]= {}
```

The following statement produces all eight variables in the order:

$\{"n", "p", "N_S^+", "N_S^0", "N_D^+", "N_D^0", "N_A^0", "N_A^-"\}$

```
(Debug) In[46]:= ParedSelectedOrigSolutionsCrossList =
   If[ ErrorPoints == {}, SelectedOrigSolutionsCrossList,
    Map[Drop[SelectedOrigSolutionsCrossList, #] &, ErrorPoints]];
```

www.manaraa.com

```
(Debug) In[47]:= solCrossOrigEqList = Map[{#[[1,2]], {#[[2,1]], #[[2,2]],
            #[[2,5]], NS - #[[2,5]],
            ND - #[[2,4]], #[[2,4]],
            #[[2,3]], NA - #[[2,3]]}} &,
         ParedSelectedOrigSolutionsCrossList];

(Debug) In[48]:= solCrossOrigEqListNoUnits = Map[{#[[1]], #[[2]]} &, solCrossOrigEqList];
```

Create a list of things that Dr. Reshchikov wants for Kaleidagraph.These are:
{"i","t", "DA", "eA", "DA+eA", "x", "1-x", "y", "z", "a4-z", "u", "w", "a6-w", "S"}
{"i", "1000 Kelvin/T", "DA", "eA", "DA +eA", "NS+", "NS0", "n", "NA0", "NA-", "p", "ND+", "ND0","S"}
Our list has: {"n", "p", "N_S^+", "N_S^0", "N_D^+", "N_D^0", "N_A^0", "N_A^-"}

```
(Debug) In[49]:= KlgraphData = MapIndexed[{#2[[1]], #1[[1]], CDA #1[[2,6]] #1[[2,7]] / GL , CnA #1[[2,1]] #1[[2,7]] / GL ,
            CDA #1[[2,6]] #1[[2,7]] / GL + CnA #1[[2,1]] #1[[2,7]] / GL , #1[[2,3]], #1[[2,4]], #1[[2,1]], #1[[2,7]],
            #1[[2,8]], #1[[2,2]], #1[[2,5]], #1[[2,6]], CnD CpS / (CpA CnS)} &, solCrossOrigEqList];


(Debug) In[50]:= constantNames = Join[{"Pexc", "G", "TinvMin", "TinvMax", "TinvInc",
          "NS", "ND", "NA", "CnS", "CnD", "CpS", "CpA", "CnA", "CDA", "ED", "EA"},
        Map[Null &, Range[17, Length[KlgraphData[[All,1]]]]]];
      constantValues = Join[{Pexc, GL, TInvMin, TInvMax, TInvinc, NS, ND, NA, CnS, CnD,
          CpS, CpA, CnA, CDA, ED, EA}, Map[Null &, Range[17, Length[KlgraphData[[All,1]]]]]];
      KlgraphOutput = Transpose[Join[{constantNames, constantValues},
          Transpose[KlgraphData]]];

(Debug) In[53]:= plotsolCrossOrigEqList =
        Transpose[Map[(tinv = #[[1]]; Map[{tinv, # } &, #[[2]]]) &, solCrossOrigEqList]];
```

This is a plot of the solutions.

```
(Debug) In[78]:= ymin = 1. × 10^17;
      ymax = 1.0 × 10^18;
      curveNames = {"n", "p", "NS+", "NS0", "ND+", "ND0", "NA0", "NA-"};
      plotColors = {Red, Orange, Darker[Yellow], Green, Cyan, Blue, Magenta, Purple};
      plotLabels = {{"n", {8.5, Log[4 × 10^8]}, {0, 1}}, {"p", {6.1, Log[2.8 × 10^7]}, {0, -1}},
          {"NS+", {9, Log[1.5 × 10^13]}, {0, -1}},
          {"NS0", {5, Log[5. × 10^14]}, {0, 1}},
          {"ND+", {5, Log[1.5 × 10^17]}, {0, 1}},
          {"ND0", {9, Log[1 × 10^10]}, {0, -1}},
          {"NA0", {4, Log[1 × 10^15]}, {0, -1}},
          {"NA-", {9, Log[1 × 10^16]}, {0, -1}}
        };
      ShowLegend[
       ListLogPlot[plotsolCrossOrigEqList,
        Joined → True, PlotStyle → Map[{Thickness[0.005], #} &, plotColors],
        Frame → True, (*PlotRange→{ymin,ymax},*)
        FrameLabel → {"1000 K/T", "Concentration (cm^-3)"}, AspectRatio → 1,
        Epilog → {MapThread[Text[Style[fBox[#1[[1]]], {#2, 18}], #1[[2]], #1[[3]]] &,
            {plotLabels, Take[plotColors, 8]}]}],
       {MapThread[{Graphics[{#2, {Thickness[0.2], Line[{{-1, 0}, {1, 0}}]}}], fBox[#1]} &,
          {curveNames, plotColors}]}]
```

المنارة للاستشارات
www.manaraa.com

(Debug) Out[82]=

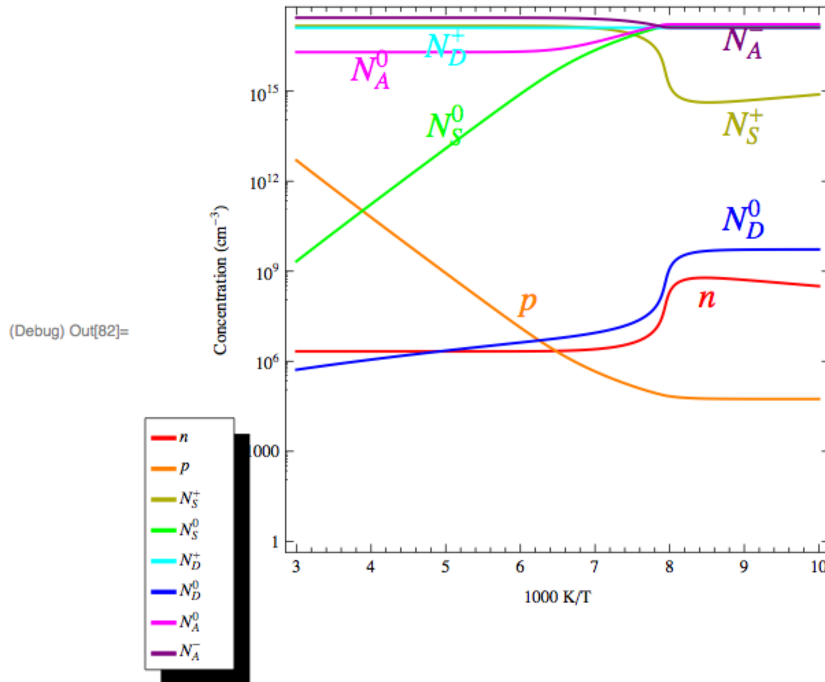

(Debug) In[62]:=

```
Revised𝒯InvList = Map[{#[[1,2]], { CDA #[[2,4]] #[[2,3]] / #[[1,2]],
      CnA #[[2,1]] #[[2,3]] / #[[1,2]] , (CDA #[[2,4]] #[[2,3]] + CnA #[[2,1]] #[[2,3]]) / #[[1,2]]}} &,
   ParedSelectedOrigSolutionsCrossList];
```

(Debug) In[63]:=

```
plotRevised𝒯InvList =
  Transpose[Map[(tinv = #[[1]]; Map[{tinv, # } &, #[[2]]]) &, Revised𝒯InvList]];
```

(Debug) In[83]:=

```
ymin = 1.0 × 10^17;
ymax = 1.0 × 10^18;
curveNames1 = {"DA", "eA", "DA+eA"};
plotColors1 = {Red, Darker[Yellow], Green};
dashingList = {Dashing[{}], Dashing[{}], Dashing[{0.1}]};
plotLabels1 =
  {{"DA", {7.1, Log[4.2 × 10^12]}, {0, 1}}, {"eA", {8.2, Log[2.8 × 10^10]}, {0, -1}},
   {"DA+eA", {5, Log[1.5 × 10^11]}, {0, -1}}
  };
ShowLegend[
 ListLogPlot[plotRevised𝒯InvList,
  Joined → True,
  PlotStyle → MapThread[{Thickness[0.005], #1, #2} &, {plotColors1, dashingList}],
  Frame → True, (*PlotRange→{ymin,ymax},*)
  FrameLabel → {"1000 K/T", "Concentration (cm^-3)"}, AspectRatio → 1,
  Epilog → {MapThread[Text[Style[fBox[#1[[1]]], {#2, 18}], #1[[2]], #1[[3]]] &,
     {plotLabels1, Take[plotColors1, 3]}]}],
 {MapThread[{Graphics[{#2, {Thickness[0.2], Line[{{-1, 0}, {1, 0}}]}}], fBox[#1]} &,
   {curveNames1, plotColors1}]}]
```

www.manaraa.com

(Debug) Out[89]=

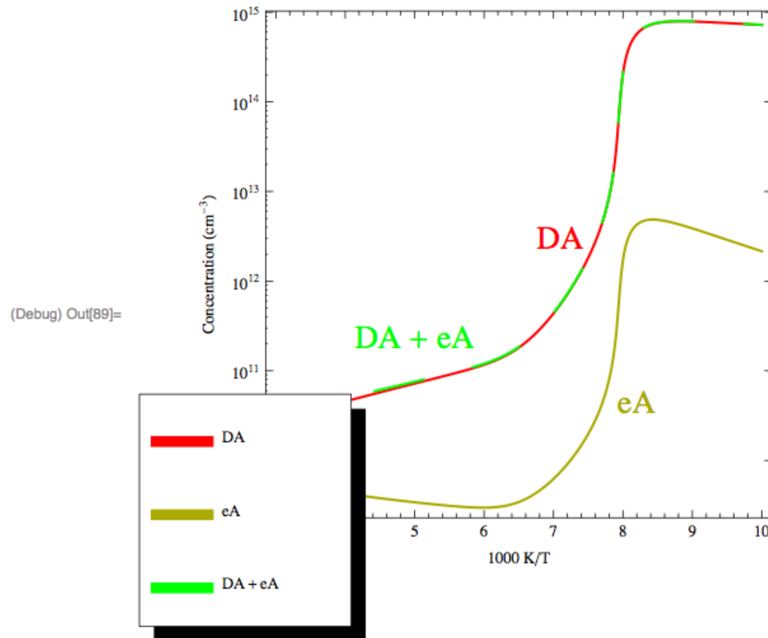

(Debug) In[71]:=
```
ExportData = Join[{{"Names", "Values", "i", "1000 Kelvin/T", "DA", "eA", "DA+eA",
    "NS+", "NS0", "n", "NA0", "NA-", "p", "ND+", "ND0", "S"}}, KlgraphOutput];
```

(Debug) In[72]:=
```
Export["L:\\PHY\\Public\\STUDENTS\\Olsen, Anita\\Dr.
  Reshchikov\\Kaleidagraph\\trialdatamar3.txt", ExportData, "Table"]
```

(Debug) Out[72]=
```
L:\PHY\Public\STUDENTS\Olsen, Anita\Dr. Reshchikov\Kaleidagraph\trialdatamar3.txt
```

www.manaraa.com

Excitation Intensity

(Debug) In[90]:=

```
𝒯Inv = 7.0; (*inverse temperature*)
𝒯 = 1000/𝒯Inv;
𝒢LMin = 1.0 × 10^15;
𝒢LMax = 1.0 × 10^25;
𝒢LMinLog = Log[𝒢LMin];
𝒢LMaxLog = Log[𝒢LMax];
𝒢LLogInc = 0.1;
Clear[n, p, 𝒩A0, 𝒩D0, 𝒩SP];
(* we are clearing previously entered values for the variables*)
𝒢LLogList = Range[𝒢LMinLog, 𝒢LMaxLog, 𝒢LLogInc];
(* this is log(G), Range[first value, last value, increment]*)
𝒢LList = Map[Exp[#] &, 𝒢LLogList]; (* Map makes a list of G's *)
origEquationssolutionsCrossList =
  Map[Clear[n, p, 𝒩A0, 𝒩D0, 𝒩SP]; {n, p, 𝒩A0, 𝒩D0, 𝒩SP} /. NSolve[{
      origEq1[# , n , 𝒩A0, 𝒩D0 , 𝒩SP , 𝒩D,
        𝒬D[𝒯, 𝒩C[𝒯], ℰDkB, 𝒞nD, g], 𝒞nA, 𝒞nD, 𝒞nS] == 0,
      origEq2[# , p , 𝒩A0, 𝒩SP , 𝒩A, 𝒩S,
        𝒬A[𝒯, 𝒩V[𝒯], ℰAkB, 𝒞pA, g], 𝒞pA, 𝒞pS] == 0,
      origEq3[n , p , 𝒩A0,
        𝒩D0 , 𝒩SP , 𝒩A, 𝒩D] == 0,
      origEq4[n , 𝒩A0,
        𝒩D0 , 𝒩D,
        𝒬D[𝒯, 𝒩C[𝒯], ℰDkB, 𝒞nD, g], 𝒞nD, 𝒞DA] == 0,
      origEq5[n , p , 𝒩SP , 𝒩S, 𝒞nS, 𝒞pS] == 0
       (* origEq6[n ,p ,
        𝒩A0 ,𝒩D0 ,𝒩A,
        𝒬A[𝒯,𝒩V[𝒯],ℰAkB,𝒞pA,g],𝒞nA,𝒞pA,𝒞DA]==
       0 This last equation is a linear combination of other
        equations and we keep it here in case we need it. *)},
     {n, p, 𝒩A0, 𝒩D0, 𝒩SP}, WorkingPrecision → 50] &, 𝒢LList];
 (* This is where we solve the set of differential equations. NDSolve cannot deal
 with the units so we've canceled the units explicitly and the concentrations
 will come out without units, however, they are in units of cm^-3. *)
```

(Debug) In[101]:=

```
indexedorigEquationssolutionsCrossList =
  MapIndexed[{#2[[1]], #1} &, origEquationssolutionsCrossList];
```

(Debug) In[102]:=

```
SelectedOrigSolutionsCrossList =
  MapThread[{{#2[[1]], #1}, Flatten[Select[#2[[2]], #[[1]] ∈ Reals ∧ #[[1]] > 0 ∧ #[[2]] > 0 ∧ #[[3]] > 0 ∧
         #[[4]] > 0 ∧ #[[5]] > 0 ∧
         #[[3]] ≤ 𝒩A ∧ #[[4]] ≤ 𝒩D ∧
         #[[5]] ≤ 𝒩S &], 1]} &,
   {𝒢LList, indexedorigEquationssolutionsCrossList}];
```

Next we check to see if there are any temperatures for which a solution has not been found.

(Debug) In[103]:=

```
CheckErrorPoints = Select[SelectedOrigSolutionsCrossList, #[[1]] == {} &]
```

(Debug) Out[103]=

```
{}
```

(Debug) In[104]:=

```
ErrorPoints = Map[{#} &, CheckErrorPoints[[All,1,1]]]
```

(Debug) Out[104]=

```
{}
```

The following statement produces all ten variables in the order:

$\{"n", "p", "N_S^+", "N_S^0", "N_D^+", "N_D^0", "N_A^0", "N_A^-"\}$

(Debug) In[105]:=

```
ParedSelectedOrigSolutionsCrossList =
   If[ ErrorPoints == {}, SelectedOrigSolutionsCrossList,
    Map[Drop[SelectedOrigSolutionsCrossList, #] &, ErrorPoints]];
```

المنارة للاستشارات

www.manaraa.com

```
(Debug) In[106]:= solCrossOrigEqList = Map[{#[[1,2]], {#[[2,1]], #[[2,2]],
          #[[2,5]], NS - #[[2,5]],
          ND - #[[2,4]], #[[2,4]],
          #[[2,3]], NA - #[[2,3]]}} &,
     ParedSelectedOrigSolutionsCrossList];

(Debug) In[107]:= solCrossOrigEqListNoUnits = Map[{#[[1]], #[[2]]} &, solCrossOrigEqList];
```

Create a list of things that Dr. Reshchikov wants for Kaleidagraph.These are:
{"i", "G", "DA","eA","DA+eA","NS+", "NS0", "n", "NA0","NA-", "p", "ND+", "ND0","S"}
Our list has: {"n", "p", "N_S^+", "N_S^0", "N_D^+", "N_D^0", "N_A^0", "N_A^-",}

```
(Debug) In[108]:= KlgraphData = MapIndexed[{#2[[1]], #1[[1]], CDA #1[[2,6]] #1[[2,7]] / #1[[1]], CnA #1[[2,1]] #1[[2,7]] / #1[[1]],
       (CDA #1[[2,6]] #1[[2,7]] + CnA #1[[2,1]] #1[[2,7]]) / #1[[1]], #1[[2,3]], #1[[2,4]], #1[[2,1]], #1[[2,7]],
       #1[[2,8]], #1[[2,2]], #1[[2,5]], #1[[2,6]], CnS #1[[2,3]] #1[[2,1]]} &, solCrossOrigEqList];

(Debug) In[109]:= constantNames =
   Join[{"T", "TInv", "GLMin", "GLMax", "GLLogInc", "NS", "ND", "NA", "CnS", "CnD", "CpS",
     "CpA", "CnA", "CDA", "ED", "EA"}, Map[Null &, Range[17, Length[KlgraphData[[All,1]]]]]];
  constantValues = Join[{T, TInv, GLMin, GLMax, GLLogInc, NS, ND, NA, CnS, CnD, CpS,
     CpA, CnA, CDA, ED, EA}, Map[Null &, Range[17, Length[KlgraphData[[All,1]]]]]];
  KlgraphOutput = Transpose[Join[{constantNames, constantValues},
     Transpose[KlgraphData]]];

(Debug) In[112]:= plotsolCrossOrigEqList =
   Transpose[Map[(GLvalue = #[[1]]; Map[{GLvalue, # } &, #[[2]]]) &, solCrossOrigEqList]];

(Debug) In[113]:= curveNames = {"n", "p", "N_S^+", "N_S^0", "N_D^+", "N_D^0", "N_A^0", "N_A^-"};
  plotColors = {Red, Orange, Darker[Yellow], Green, Cyan, Blue, Magenta, Purple};
  plotLabels = {{"n", {6.85, Log[4 × 10^11]}, {0, 1}}, {"p", {6.8, Log[2.8 × 10^7]}, {0, -1}},
     {"N_S^+", {6.8, Log[2.8 × 10^14]}, {0, -1}},
     {"N_S^0", {6.9, Log[2. × 10^17]}, {0, 1}},
     {"N_D^+", {6.6, Log[2.5 × 10^17]}, {0, 1}},
     {"N_D^0", {6.8, Log[2.8 × 10^12]}, {0, -1}},
     {"N_A^0", {6.6, Log[2.5 × 10^17]}, {0, 1}},
     {"N_A^-", {6.8, Log[2.8 × 10^12]}, {0, -1}}
    }; (* To place the labels in the correct location, since we have a semi-log plot,
  the vertical position is given by the natural log of the value. *)
  ShowLegend[ListLogPlot[plotsolCrossOrigEqList,
     Joined → True, PlotStyle → Map[Directive[{Thickness[0.005], #}] &, plotColors],
     (* Map is a shortcut to change all of the line
      thicknesses instead of each one individually. *)
     Frame → True,
     FrameLabel → {"G", "Concentration (cm^-3)"}, AspectRatio → 1, (* The AspectRatio
      defines the proportions (vertical to horizontal) of the image *)
     Epilog → {MapThread[Text[Style[fBox[#1[[1]]], {#2, 18}], #1[[2]], #1[[3]]] &,
        {plotLabels, Take[plotColors, 8]}],
       Thickness[0.005], Dashing[0.02],
       Line[{{6.58, 0}, {6.58, 1. × 10^20}}]}],
    (* Epilog is performed after the plot is done,
    adding labels to the curves. fBox is a function that we came up with to
     make the labels look like they are in mathematical notation. This is
     defined at the very top of the file. #1[[1]] takes just the title of the
     three quantities in each element. {#2,18} is the plot colors and the size
     of the font. #1[[2]] gives the position of the label and #1[[3]] tells how the
     label is positioned relative to the coordinate. The last part of this
     command draws the vertical dashed line at the crossover temperature. *)
    {MapThread[{Graphics[{#2, {Thickness[0.2], Line[{{-1, 0}, {1, 0}}]}}], fBox[#1]} &,
      {curveNames, plotColors}]}]; (* This last part is manipulating
   the legend because the default gives an unacceptable format. *)
```

This is a plot of the solutions.

المنارة للاستشارات

www.manaraa.com

```
(Debug) In[116]:= ymin = 1.0 × 10^17;
ymax = 1.0 × 10^18;
curveNames = {"n", "p", "N_S^+", "N_S^0", "N_D^+", "N_D^0", "N_A^0", "N_A^-"};
plotColors = {Red, Orange, Darker[Yellow], Green, Cyan, Blue, Magenta, Purple};
plotLabels = {{"n", {6.85, Log[4 × 10^11]}, {0, 1}}, {"p", {6.8, Log[2.8 × 10^7]}, {0, -1}},
    {"N_S^+", {6.4, Log[1.5 × 10^17]}, {0, -1}},
    {"N_S^0", {6.9, Log[5. × 10^17]}, {0, 1}},
    {"N_D^+", {6.4, Log[2.45 × 10^17]}, {0, 1}},
    {"N_D^0", {6.8, Log[2.8 × 10^12]}, {0, -1}},
    {"N_A^0", {6.7, Log[8. × 10^17]}, {0, -1}},
    {"N_A^-", {6.7, Log[2.55 × 10^17]}, {0, -1}}
   };
ShowLegend[
 ListLogLogPlot[plotsolCrossOrigEqList,
  Joined → True, PlotStyle → Map[{Thickness[0.005], #} &, plotColors],
  Frame → True, (*PlotRange→{ymin,ymax},*)
  FrameLabel → {"𝒢", "Concentration (cm^-3)"}, AspectRatio → 1,
  Epilog → {MapThread[Text[Style[fBox[#1[[1]]], {#2, 18}], #1[[2]], #1[[3]]] &,
     {plotLabels, Take[plotColors, 8]}],
    Thickness[0.005], Dashing[0.02],
    Line[{{6.58, 0}, {6.58, 1. × 10^20}}]}],
 {MapThread[{Graphics[{#2, {Thickness[0.2], Line[{{-1, 0}, {1, 0}}]}}], fBox[#1]} &,
   {curveNames, plotColors}]}]
```

(Debug) Out[120]=

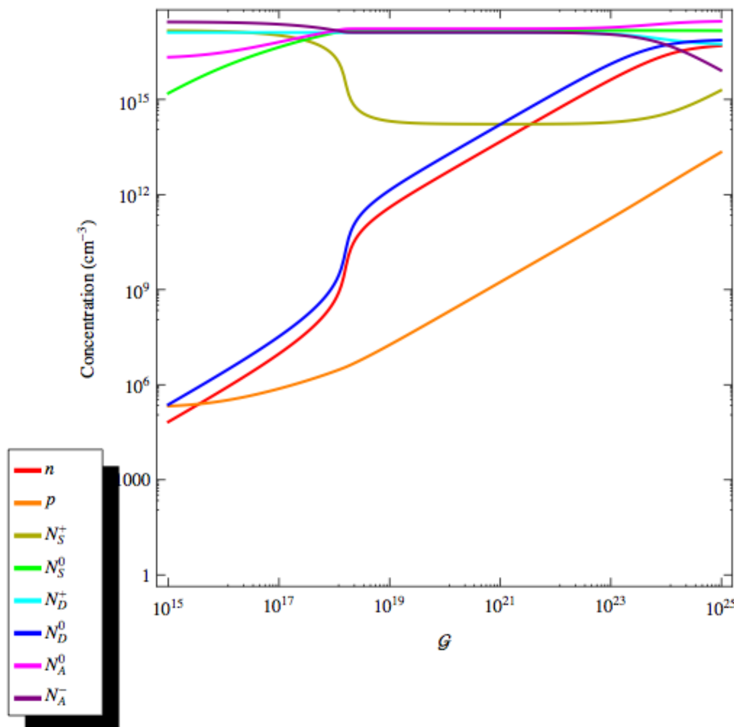

www.manaraa.com

```
(Debug) In[121]:= RevisedList = Map[{#[[1,2]], { CDA #[[2,4]] #[[2,3]] / #[[1,2]],
        CnA #[[2,1]] #[[2,3]] / #[[1,2]] , (CDA #[[2,4]] #[[2,3]] + CnA #[[2,1]] #[[2,3]]) / #[[1,2]]}} &,
     ParedSelectedOrigSolutionsCrossList];

(Debug) In[122]:= plotRevisedList =
    Transpose[Map[(𝒢Lvalue = #[[1]]; Map[{𝒢Lvalue, # } &, #[[2]]]) &, RevisedList]];

(Debug) In[123]:= ymin = 1.0 × 10^17;
ymax = 1.0 × 10^18;
curveNames2 = {"DA", "eA", "DA+eA"};
plotColors2 = {Red, Darker[Yellow], Green};
dashingList = {Dashing[{}], Dashing[{}], Dashing[{0.1}]};
plotLabels2 =
   {{"DA", {6.85, Log[4 × 10^11]}, {0, 1}}, {"eA", {6.8, Log[2.8 × 10^7]}, {0, -1}},
    {"DA+eA", {6.4, Log[1.5 × 10^17]}, {0, -1}}
   };
ShowLegend[
 ListLogLogPlot[plotRevisedList,
  Joined → True,
  PlotStyle → MapThread[{Thickness[0.005], #1, #2} &, {plotColors2, dashingList}],
  Frame → True, (*PlotRange→{ymin,ymax},*)
  FrameLabel → {"𝒢", "Concentration (cm^-3)"}, AspectRatio → 1,
  Epilog → {MapThread[Text[Style[fBox[#1[[1]]], {#2, 18}], #1[[2]], #1[[3]]] &,
      {plotLabels2, Take[plotColors2, 3]}],
     Thickness[0.005], Dashing[0.02],
     Line[{{6.58, 0}, {6.58, 1. × 10^20}}]}],
 {MapThread[{Graphics[{#2, {Thickness[0.2], Line[{{-1, 0}, {1, 0}}]}}], fBox[#1]} &,
   {curveNames2, plotColors2}]}]
```

(Debug) Out[129]=

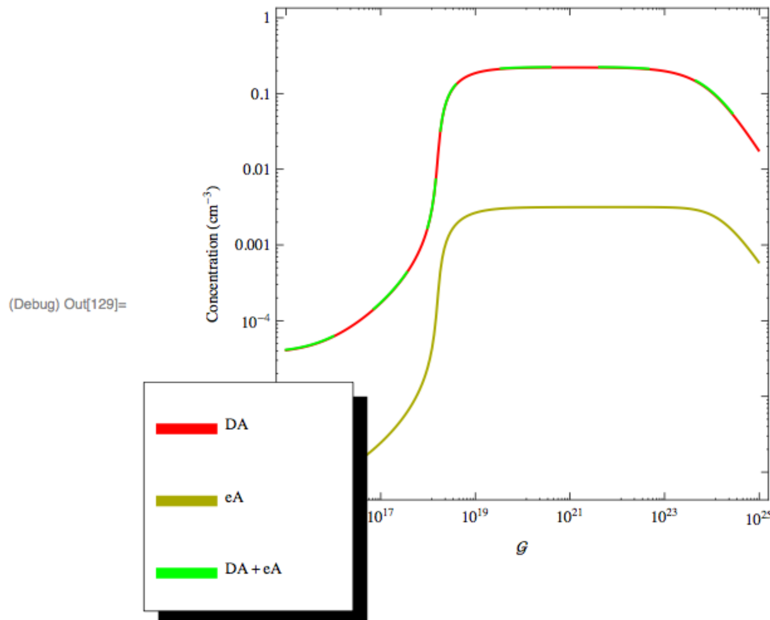


```
(Debug) In[130]:= ExportData = Join[{{"Names", "Values", "i", "G", "DA", "eA", "DA+eA", "NS+",
        "NS0", "n", "NA0", "NA-", "p", "ND+", "ND0", "S"}}, KlgraphOutput];

(Debug) In[131]:= Export["L:\\PHY\\Public\\STUDENTS\\Olsen, Anita\\Dr.
      Reshchikov\\Kaleidagraph\\march3excb.txt", ExportData, "Table"]

(Debug) Out[131]= L:\PHY\Public\STUDENTS\Olsen, Anita\Dr. Reshchikov\Kaleidagraph\march3excb.txt
```

المنارة للاستشارات

www.manaraa.com

Explanation of Mathematica Program

The Mathematica program is a useful tool in the computation of lengthy numerical calculations and graphical representation of those calculations to compare the theory of the rate equation model with graphs created directly from experimental data. Each program is titled with the specific scenario that is being taken into consideration followed by a small string of commands that provides automatic access to commonly used scientific data, such as the value of physical constants and conversions between different units, and automatic labeling of graphical lines into legends.

The first section of the program is titled **Analysis of Data** and introduces the parameters involved and how they are defined in Mathematica. The parameter values associated with a particular semiconductor are briefly introduced in the beginning of this section under the subtitle of **Parameter Values**. These parameters include defect species, concentrations of defects, capture coefficients, energy levels, effective density of states, temperature and electron-hole generation rate, and temperature factors followed by a band diagram that depicts the assumed energy states and the flow of electrons during illumination.

The following subsection of **Defining Parameters in *Mathematica*** inputs the numerical data of these parameters into the program for analysis. The values of the defect concentrations of N_A, N_D, and N_S are given in units cm^{-3} and are entered into the program as constants labeled *N**A***, *N**D***, and *N**S*** with charge states that are later introduced in the program as *N**AO***, *N**AM***, *N**DO***, *N**DP***, *N**SO***, and *N**SP***, where ***M*** stands for "minus" and ***P*** stands for "plus". The capture coefficient values are in units of cm^3/s and are entered as constants consisting of C_{nA}, C_{nD}, C_{nS}, C_{pA} and C_{pS} that are symbolized in the Mathematica program as *C***nA**, *C***nD**, *C***nS**, *C***pA** and *C***pS.**

المنارة للاستشارات
www.manaraa.com

These are followed by temperature (in Kelvins) dependent functions of the effective density of states in the conduction and valence bands and are represented in units of cm^{-3} along with the degeneracy factor represented as *N**C***, *N**V*** and ***g***, respectively. Since the effective mass of the electron and hole are known for GaN, the effective density of states is entered into Mathematica as the functions of

$$N_C = 1.57 \times 10^{19} \left(\frac{T}{10^3} \right)^{3/2} \tag{24}$$

$$N_V = 1.00 \times 10^{20} \left(\frac{T}{10^3} \right)^{3/2} \tag{25}$$

and the degeneracy factor is two, to account for the electron spin.

The values of the energy levels of acceptors E_A and donors E_D in units of meV are also included in this section and are labeled as ***EA*** and ***ED***. For simplification purposes the following functions are defined in Mathematica:

$$EAkB = \frac{E_A}{k_B(1000K)} \tag{26}$$

$$EDkB = \frac{E_D}{k_B(1000K)} \tag{27}$$

so that when they are multiplied by the product of inverse temperature and 1000 Kelvin (denoted by $Tinv = \frac{1000K}{T}$ in Mathematica) they give energy divided by k_BT. The Boltzmann's constant is obtained from a Physical Constants package, loaded at the beginning of the Mathematica program, and the units of these equations are converted to one to ease numerical computation by using unitless numbers.

المنارة للاستشارات

www.manaraa.com

The simplified Eqs. (26) and (27) are then used in our temperature factors of Q_A and $Q_{D,}$ These are functions dependent on the variables of temperature and density of states, which is also dependent on temperature, and are represented as ***QA*** and ***QD***. Semi-log plots of Q_D and Q_A versus 10^3 K/T are displayed to show how the rate changes with temperature.

The following section, **Thermal Effects**, gives a brief explanation of the defect species. This is followed by the introduction of the rate equations for the band diagram displayed in this section, in **Error! Reference source not found.**, and these functions are entered into the program under the subsection title of **Defining Rate Equations in *Mathematica***. The equations are rewritten so that zero is on the right hand side and, since the sum of the charge states for each level is previously undefined, they are now defined in a module that precedes the equation to make use of them in these functions.

The next subsection in this section is **Calculation of carrier densities over a temperature range**, where the effect of temperature on concentrations at different levels and PL intensity is calculated and shown in subsequent graphs. For the numerical calculations, a range of temperature (given in inverse temperature) and increments is entered into the program. The variables of *n*, *p*, ***NAO***, ***NDO***, and ***NSP*** are cleared of any previously stored values and lists of inverse temperature and temperature in Kelvins is set up for graphical interpretation. The excitation intensity and generation rate in terms of the excitation intensity are then entered as constants. This is followed by a line of code used to solve the set of differential equation. An indexed cross list is then generated by the program to number the solutions so that solutions that were not produced can be identified. The next line of code selects all solutions for which all the concentrations have physically reasonable values. A statement to check if there are any temperatures for which a solution has not been found follows this.

www.manaraa.com

Now that the program has gathered all reasonably sound solutions for our differential equations, concentrations are listed in an order that is convenient for graphing purposes and for exporting data into Kaleidagraph program for comparison with experimental data. This is followed by a graph of concentration versus inverse temperature and a graph of PL intensities versus inverse temperature.

Since the excitation rate may remain constant or vary depending on experimental focus, it is entered as a constant in the **Calculations of carrier and densities over a temperature range** section and remains a variable that is observed over a specific range in the section titled **Excitation Intensity**. The temperature is held as a constant here, and the procedure of finding reasonable solutions, as seen in the temperature range section of this program, and exporting arranged lists into Kaleidagraph for comparison, is repeated here for an excitation range. This is followed by a graph of concentration versus excitation and a graph of PL intensities versus excitation.

المنارة للاستشارات

www.manaraa.com